Spectroscopy to Support Short Wavelength Light Source Development

Gerry O'Sullivan

University College Dublin

Solvay Workshop Brussels, November 25-27 2019

Collaborators

UCD
Kevin Carroll
Padraig Dunne
Emma Sokell
Fergal O'Reilly
Paddy Hayden
Tom McCormack
Nicola Murphy
Ronan Faulkner
Anthony Cummings
Deirdre Kilbane
Rebekah D'Arcy
John Sheil
Takamitsu Otsuka
Takanori Miyazaki
Luning Liu
John White

DCU
John Costello

Utsunomiya
Takeshi Higashiguchi
Goki Arai
Thanh-Hung Dinh
Hiroyuki Hara
Yoshiki Kondo
Yuhei Suzuki,
Toshiki Tamura
Takuya Gisuji
When-Bo Chen

NIFS
Chihiro Suzuki
Takako Kato
Daiji Kato
Izumi Murakami
Hiroyuki Sakaue

Wuhan
Tao Wu

Lanzhou University
Bowen Li

NWNU Lanzhou
Chenzhong Dong
Maogen Su

NIST
John Gillaspy
Yuri Ralchenkpo
Joe Reader

Kansai QSI
Akira Sasaki

CTU Prague
Jiri Lampouch
Ladislaw Pina
Akira Endo
Ragava Lokasani
Elle Floyd Barte

TMU
Hajime Tanuma
Naoki Namudate

Toyama
Hayato Ohashi

ILE Osaka
Katsunobu Nishihara
Hiroaki Nishimura
Shinsuke Fujioka
Atsushi Sunahara

Outline

- Applications of Laser Produced Plasmas (LPPs) as Light Sources for Lithography and Microscopy.
- Properties of LPPs
- Properties of $\Delta n = 0$ UTAs
- Application of $\Delta n = 1$ UTAs
- Conclusions/Outlook

Lithography and Moore's Law

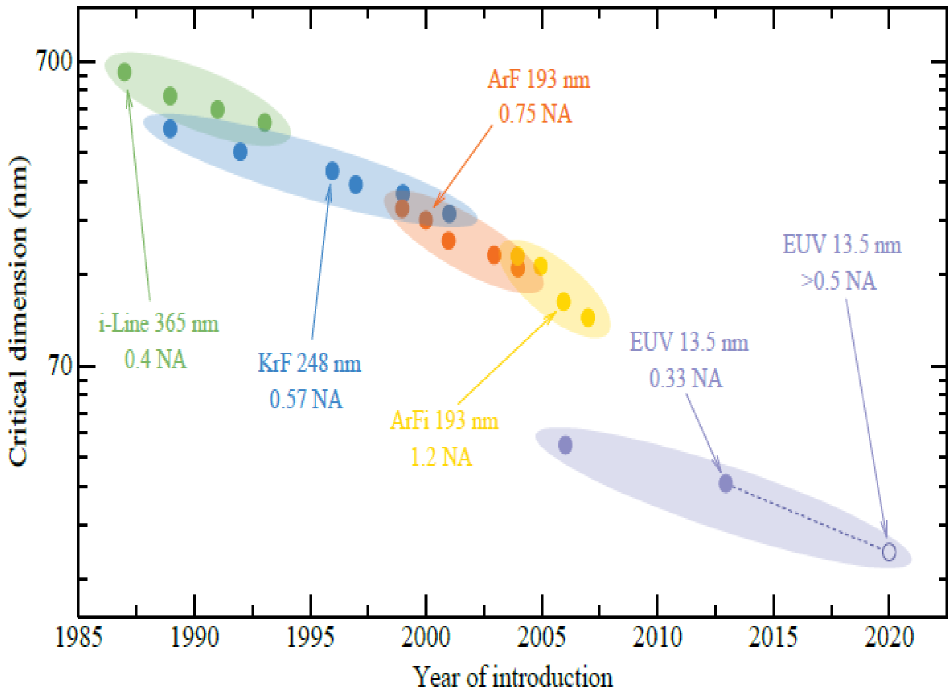

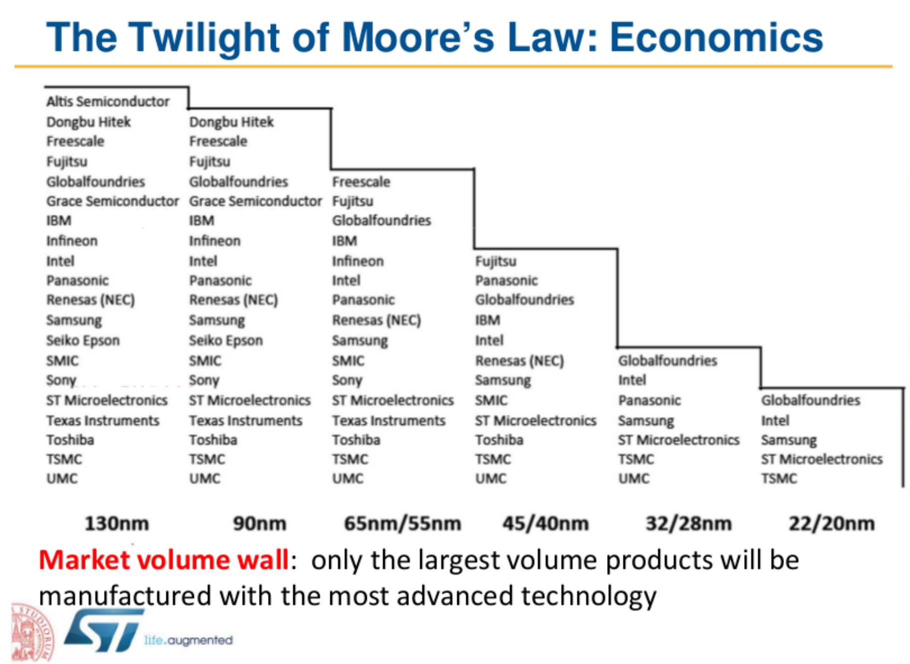

Number of transistors doubles approximately every 18 months

Predicated on decrease in feature size

Photolithographic Principle

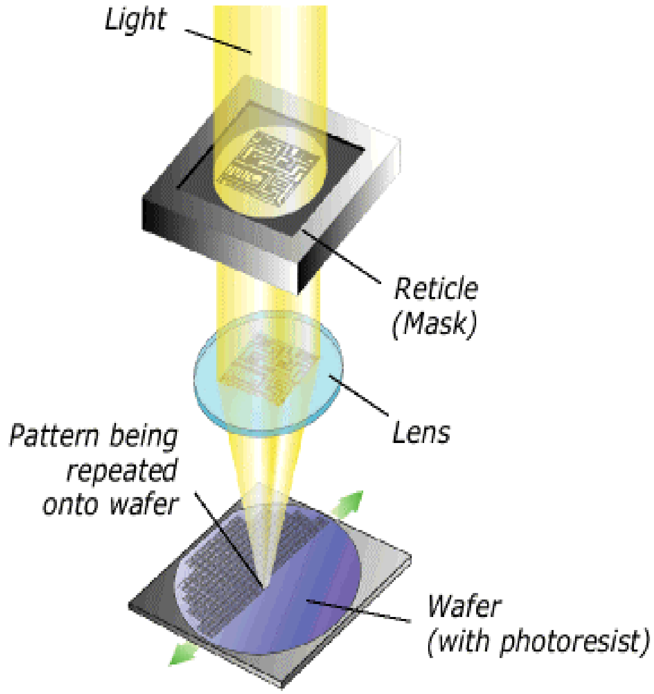

EUVL must use reflective optics

Diffraction limited resolution/ Rayleigh criterion. Smallest feature size

$$\Delta x = k\lambda/NA$$

$$NA = n\sin\vartheta$$

To achieve smaller structures: Higher NA

- Immersion
- Optimise k factors
- Double Patterning
- Multiple Patterning
- Reduce source wavelength

Evolution of Lithography Wavelength

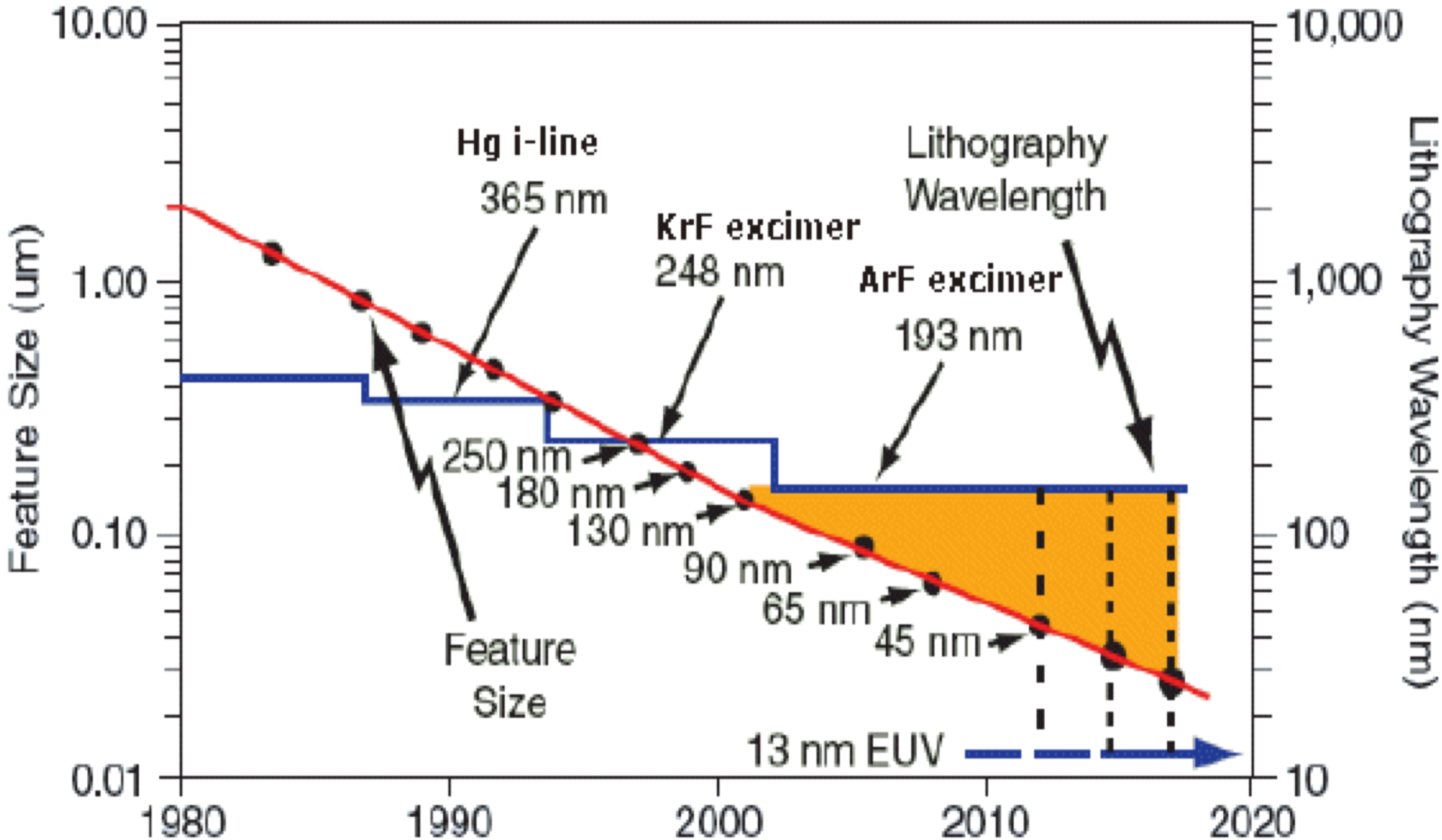

Why 13.5 nm Lithography?

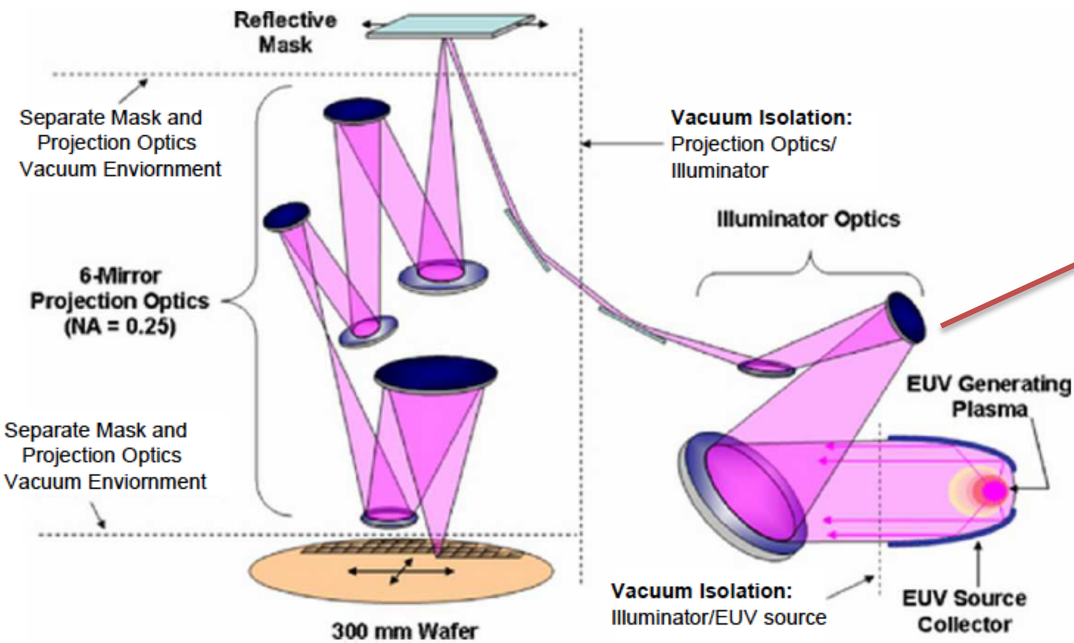

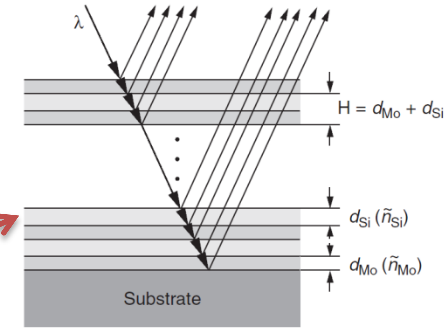

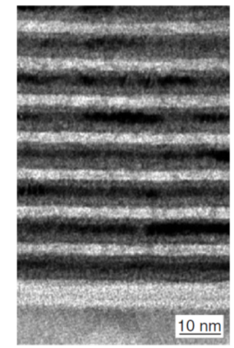

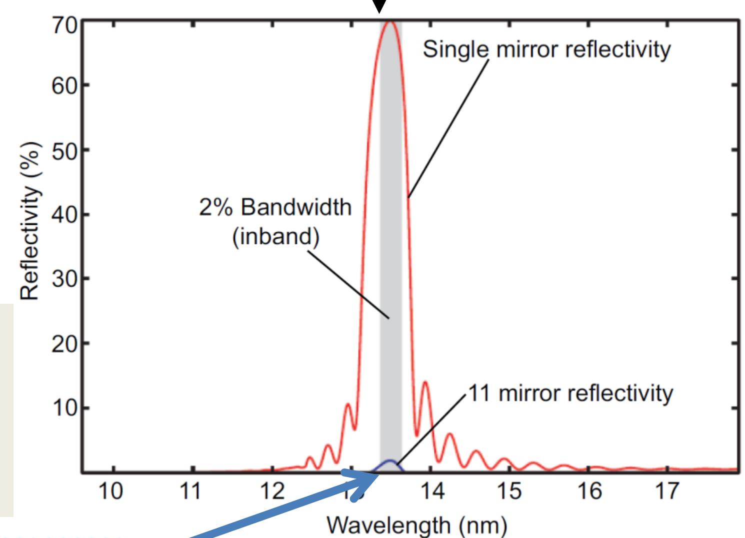

"http://www.dcsc.tudelft.nl/~mverhaegen/n4ci/pid.htm,"
P. Hayden, PhD thesis, UCD, 2007.
B. Wu and A. Kumar, Extreme Ultraviolet Lithography, McGraw-Hill Professional, 2009.

Source Power Requirement
@ Intermediate Focus~ 250 W
=1.7 x 10^{19}photons/s

EUV light transmittance is only 2% with 11 reflection mirror systems

Target Geometry (Mass-limited tin Droplet Targets)

At high repetition rates, it is not possible to use solid (slab) targets.

For EUV, rep. rate $=10^5$ Hz

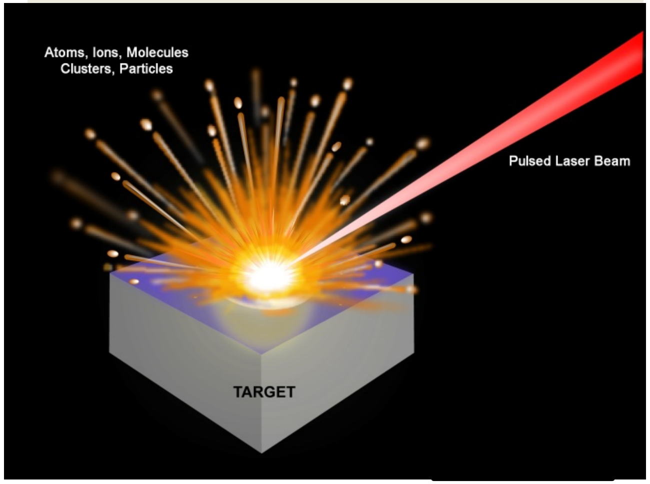

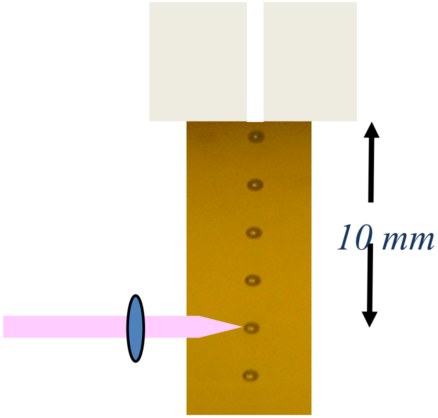

Martin Richardson et al.

Target should be fully ionized by end of laser pulse.

Low mass Sn content. number of Sn atoms should be equal to number of radiators.

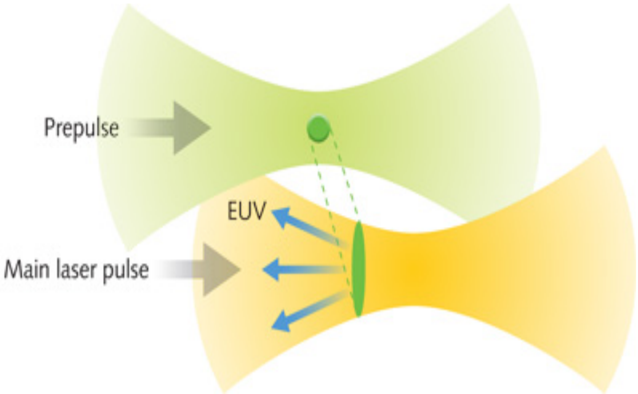

Plasma located far from nozzle. Ideally, no nozzle erosion.

Commercial Laser Produced Plasma Sources

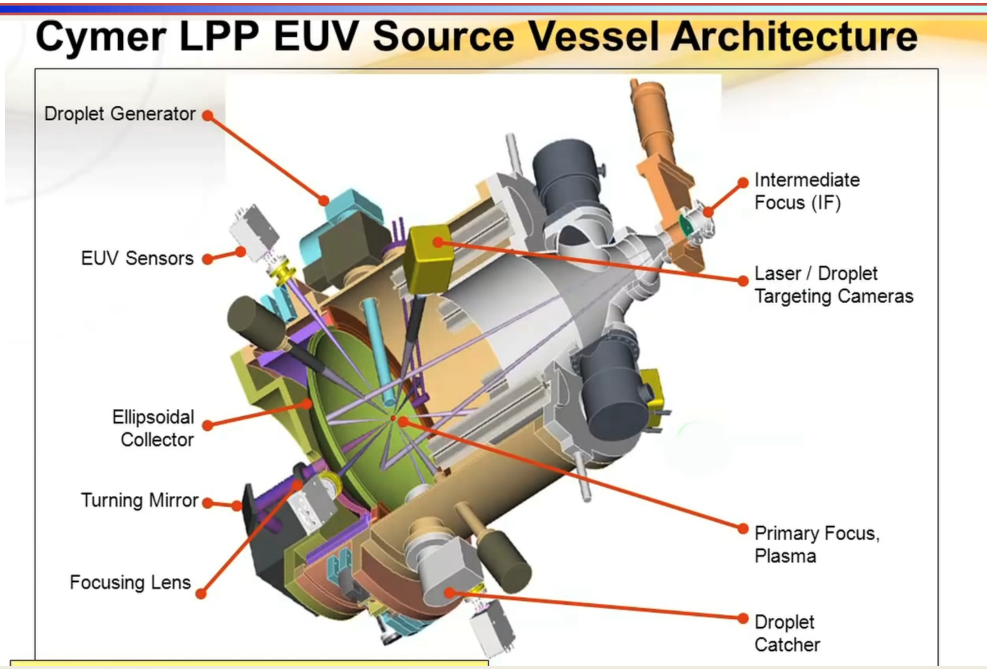

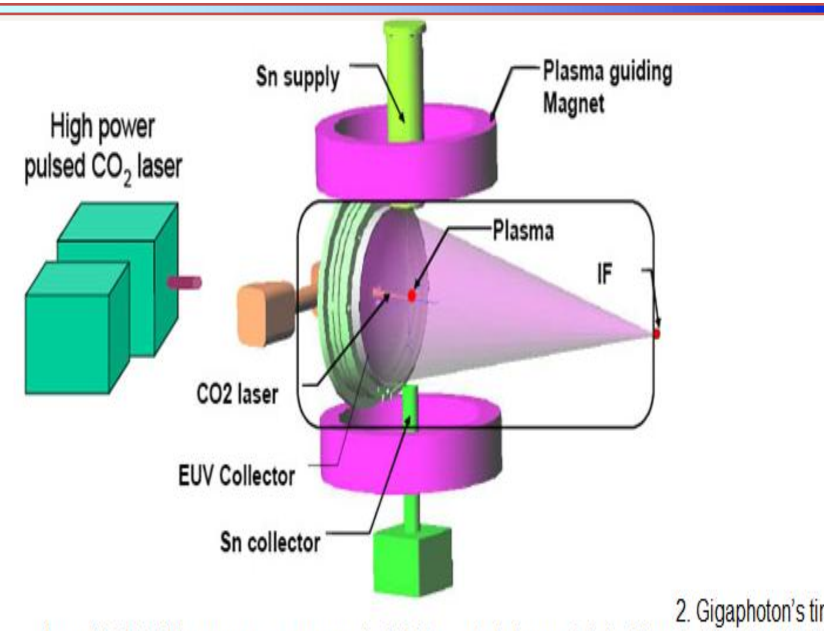

Schematic of Gigaphoton Source

- Gigaphoton and CYMER have obtained > 250 W at Intermediate focus.
- Gigaphoton:Nd:YAG prepulse, CO_2 main pulse, Cymer CO_2 main and pre-pulse.
- Target should be fully ionized by end of laser pulse
- Problems: Droplet stability, CO_2 beam quality.

Progress in CE

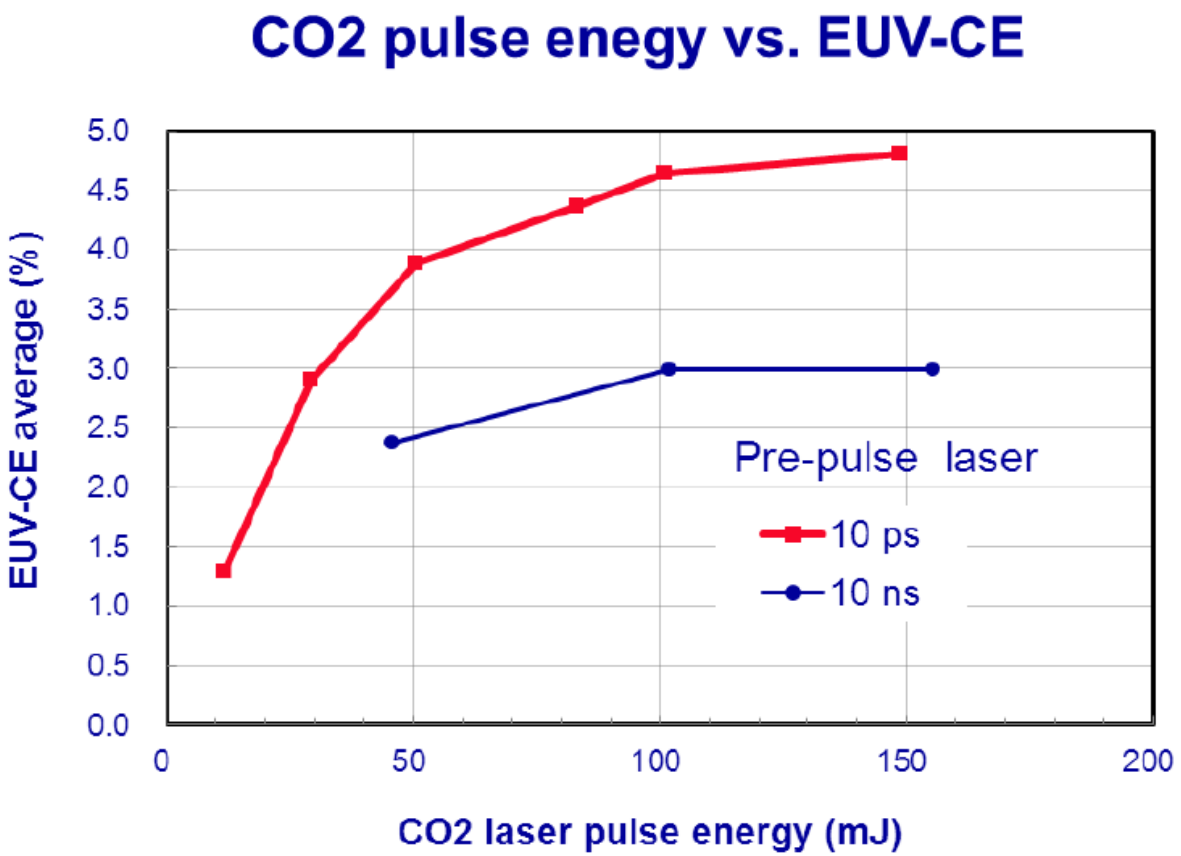

Mizoguchi Proc.2016 International Workshop on EUV Lithography http://www.euvlitho.com/2016/2016%20EUVL%20Workshop%20Proceedings.pdf

Source Power Progress

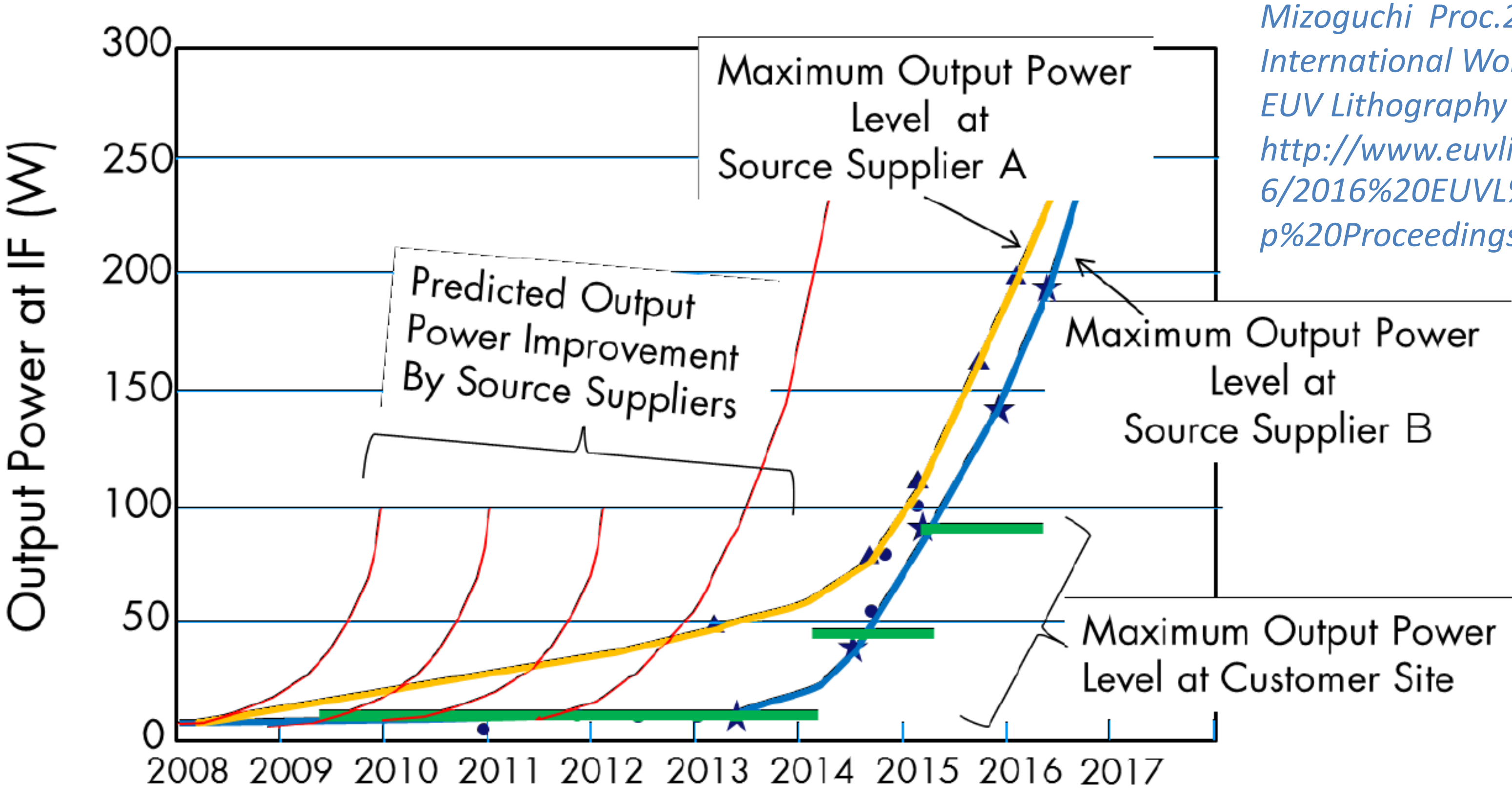

Mizoguchi Proc.2016 International Workshop on EUV Lithography http://www.euvlitho.com/2016/2016%20EUVL%20Workshop%20Proceedings.pdf

Gigaphoton: 188 W for 7 hrs (April 2016) Maximum power 264W @CE 0f 4% （In-burst mode, 27 kW CO_2 laser @ 100kHz)

~5.5% CE with ~30 µm droplet target

Commercial EUV Tool (ASML)

http://www.semiwiki.com/forum/content/1466-extreme-ultra-violet-euv.html

Water window source development

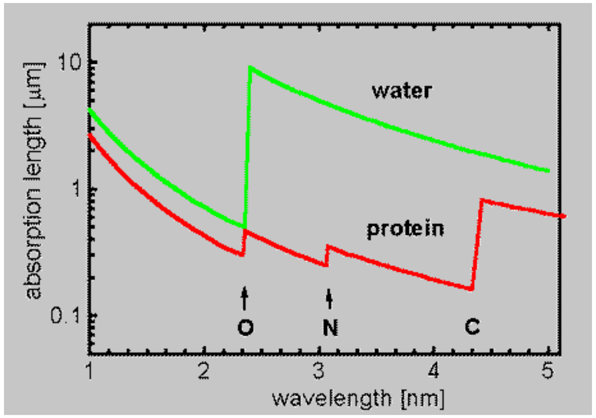

Water window : 2.34-4.38 nm.

Relative transparency of water allows investigation of biomolecules, cells and proteins in their natural aqueous environment by x-ray transmission microscopy or tomography

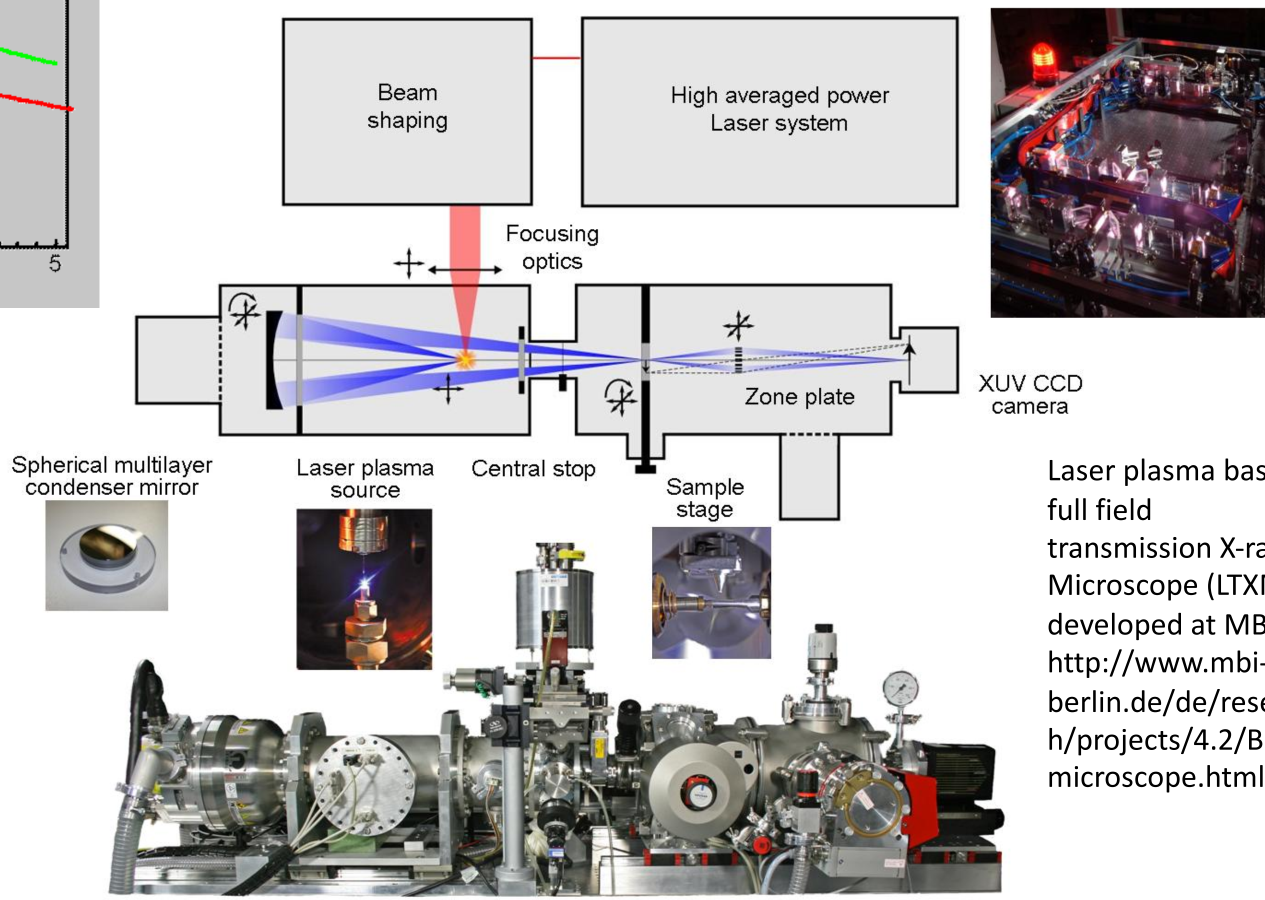

Laser plasma based full field transmission X-ray Microscope (LTXM) developed at MBI. http://www.mbi-berlin.de/de/research/projects/4.2/BLIX/microscope.html

SXR Tomography: Zone Plate Optics

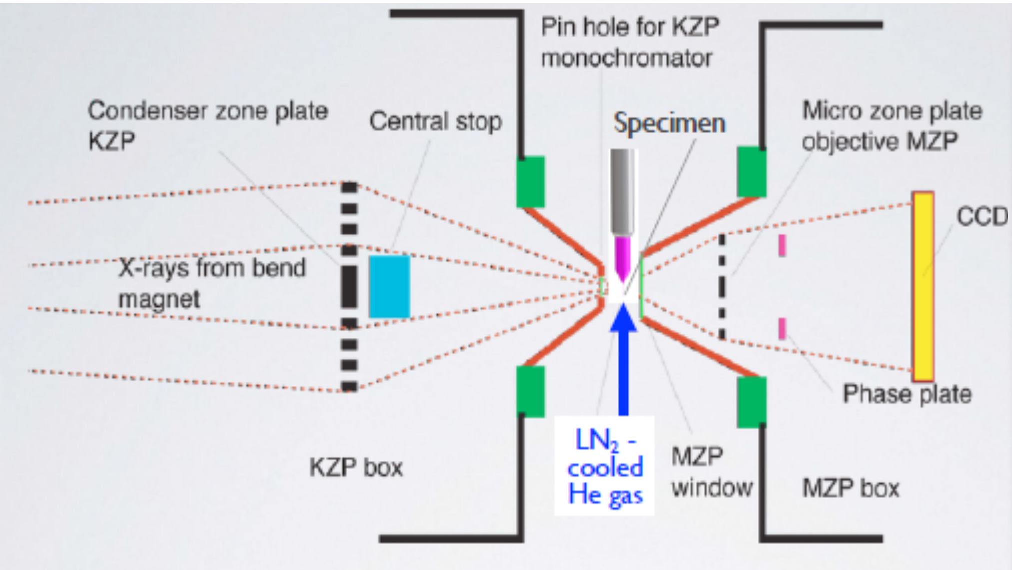

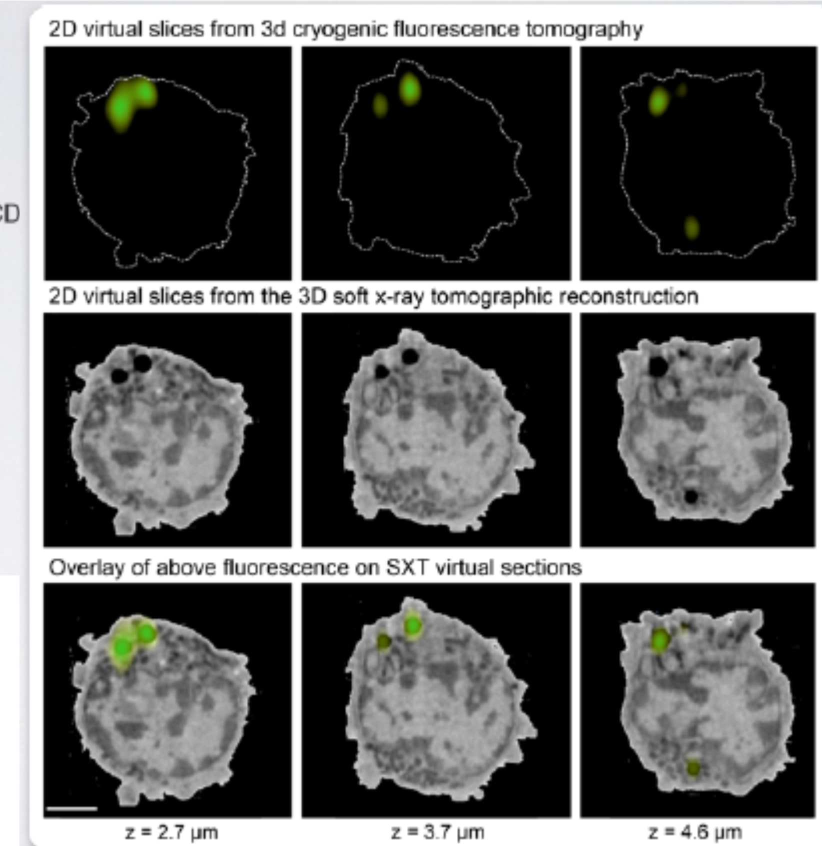

Mouse olfactory epithelium

~ 1400 genes for olfaction in mice; each cell expresses just one

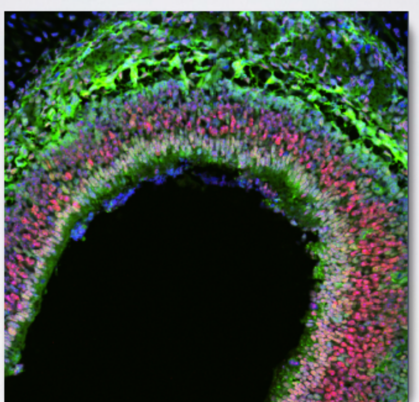

Stavros Lomvardas, UCSF

Smith EA, McDermott G, Do M, Leung K, Panning B, Le Gros MA and Larabell CA (2014). Quantitatively imaging chromosomes using correlated cryo-fluorescence and soft x-ray tomographies. *Biophysical Journal.* 107(8) 1988-96.

Multilayer mirrors in the EUV/SXR

Material	Wavelength (nm)	Reflectivity (%)
Cr/V	2.42	9
Cr/Ti	2.73	17
TiO_2/ZnO	2.74	29
Cr/Sc	3.12	32
Cr/Sc	3.14	21
Cr/Sc B_4C	3.15	32.1
Cr/Sc	3.35	10
Cr/Sc	3.37	5.5

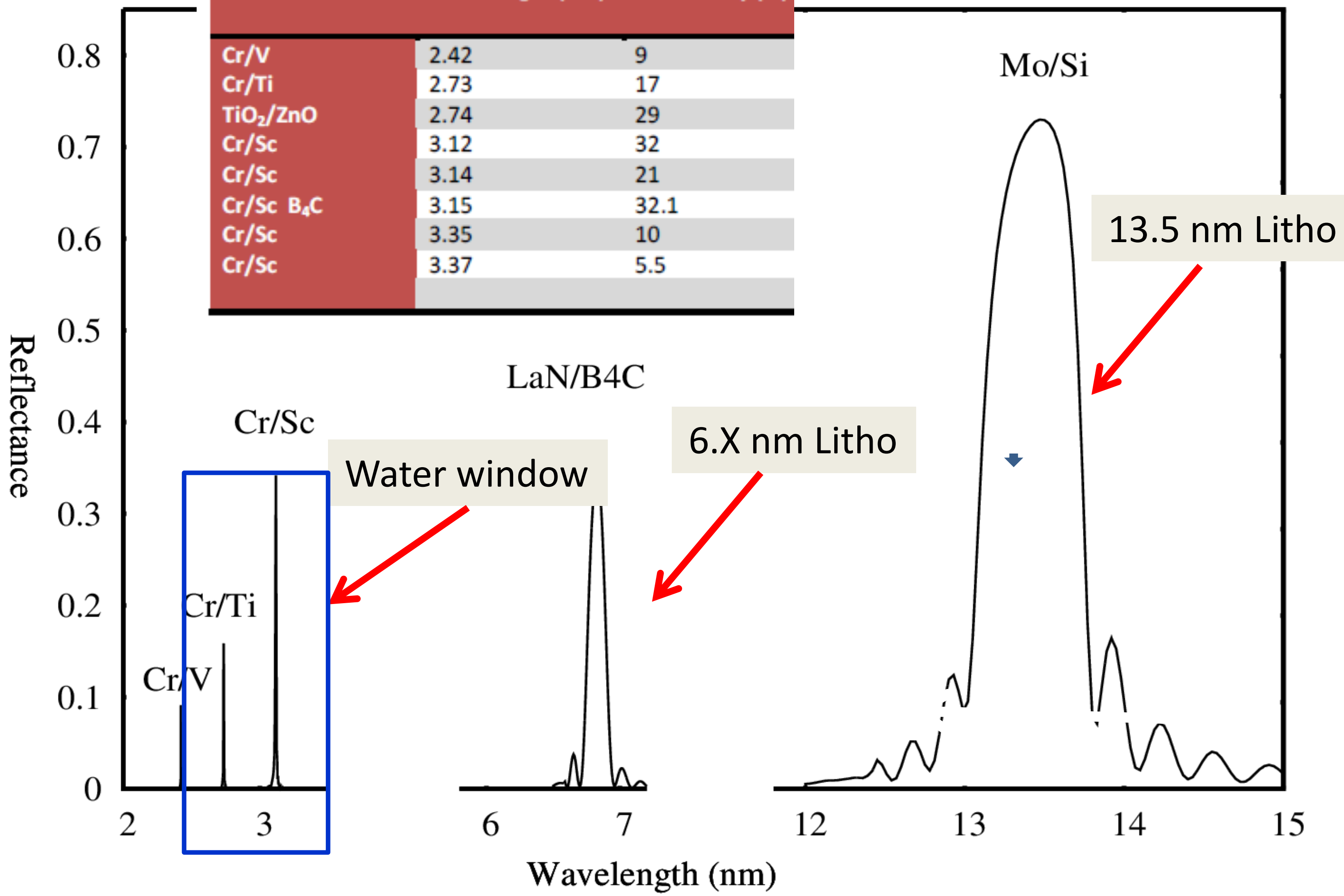

Outline

- Applications of Laser Produced Plasmas (LPPs) as Light Sources for Lithography and Microscopy.
- Properties of LPPs
- Properties of $\Delta n = 0$ UTAs
- Application of $\Delta n = 1$ UTAs
- Conclusions

Laser produced plasmas (LPPs)

Expansion velocity ≈ 10^6 - 10^7 cms^{-1}

For ns duration plasmas Collisional Radiative (CR) Equilibrium assumed

Average charge

≈ 0.67 $(ZT_e)^{1/3}$

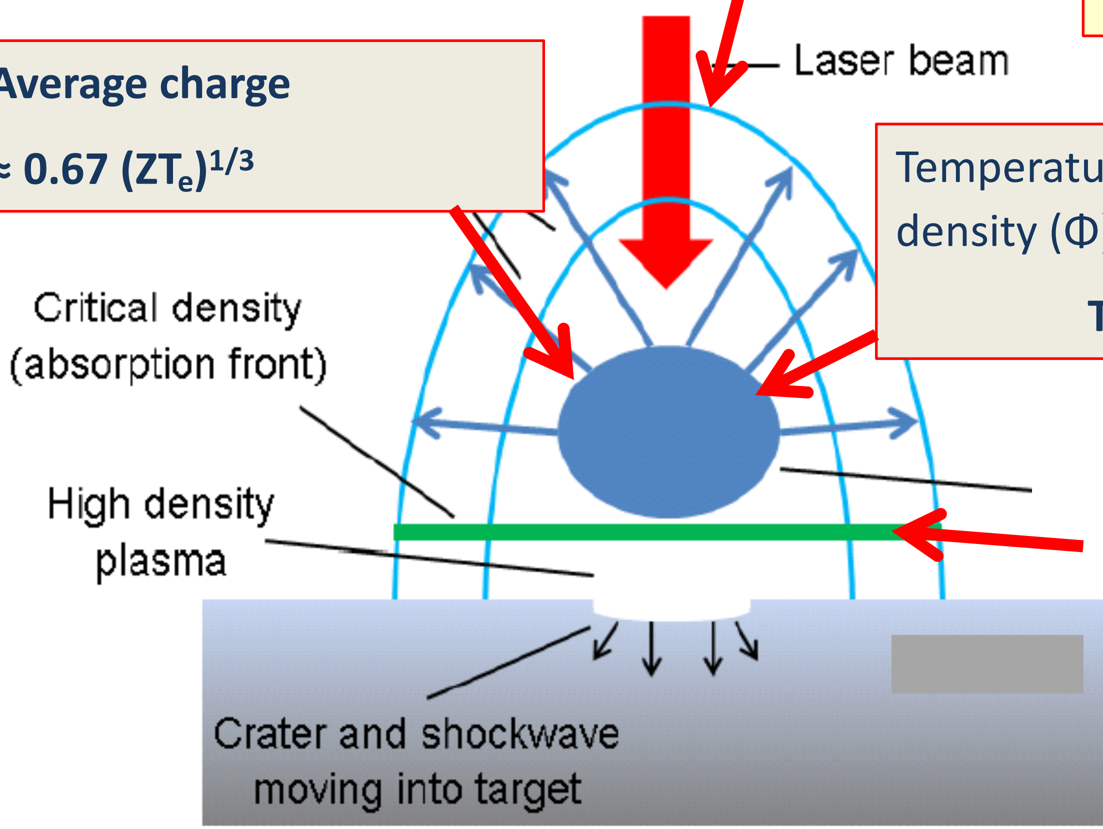

Temperature depends on laser power density (Φ),

T_e(eV) α $(\lambda^2\Phi)^{3/5}$ …CR model

Critical electron density,

n_{ec} $=10^{19} – 10^{21}$ cm^{-3}

depends on laser wavelength

(n_{ec}~[$10^{21}/\lambda(\mu m)^2$] cm^{-3})

Effect of Increasing Power Density Φ

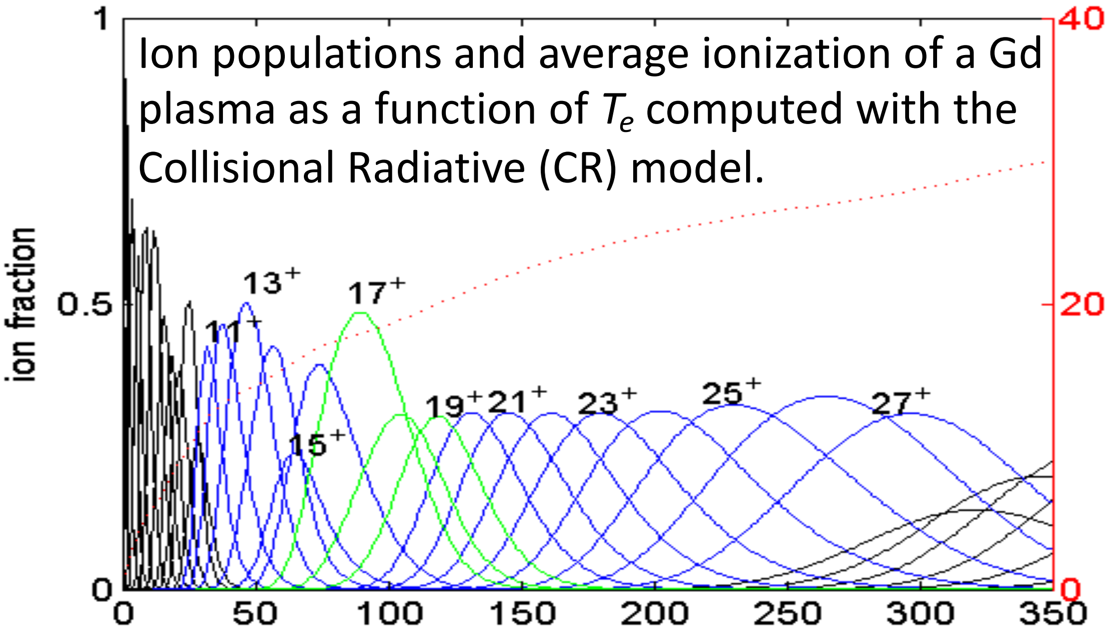

Increasing charge state requires higher power density and tighter focussing that causes increased kinetic losses due higher temperature. Therefore, high power density usually means tighter focus, Increased kinetic loss due to lateral expansion.

Competition between kinetic and radiative losses.

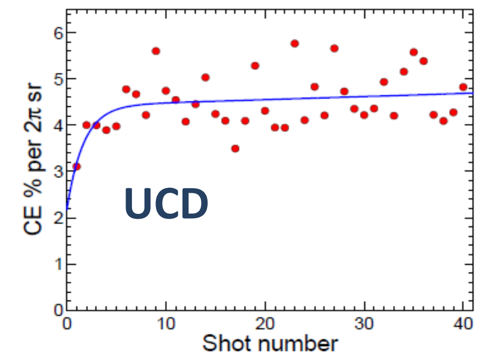

CE for Sn increased after multiple exposures on same target position

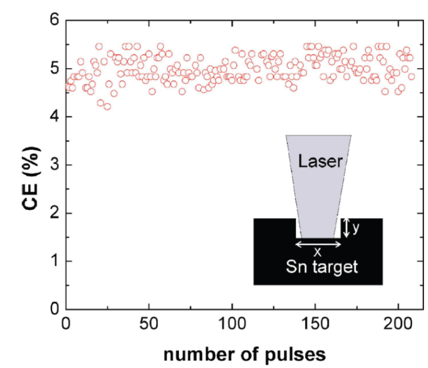

Harilal *et al* used a CO_2 pulse with $\tau = 25$ - 55ns
Typically FWHM = 30 ns, $\Phi = 6 \times 10^9$ Wcm^{-2}

Energy Losses

Plasma expansion:

Fastest and most highly charged ions at centre of the plume.

(O'Connor et al. 2011, JAP 109,, 073301)

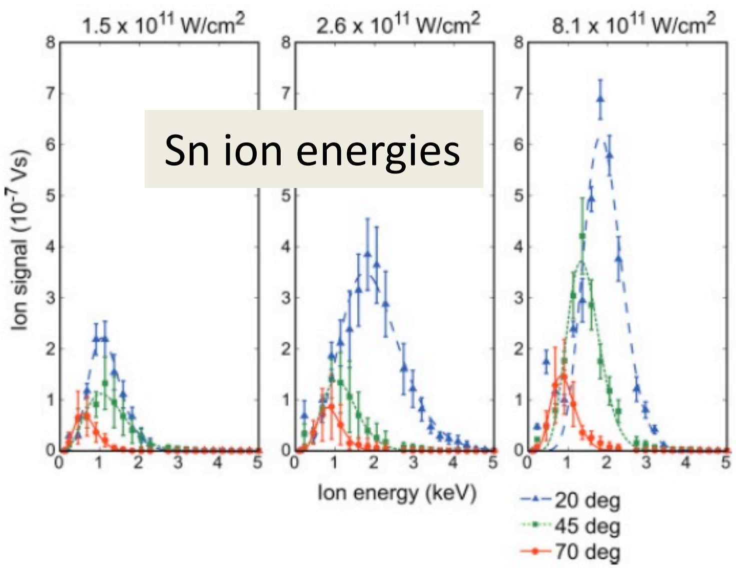

Expansion velocity increases with Φ.

Reduce by reducing Φ or by reducing shock wave momentum (target density)

Radiation:

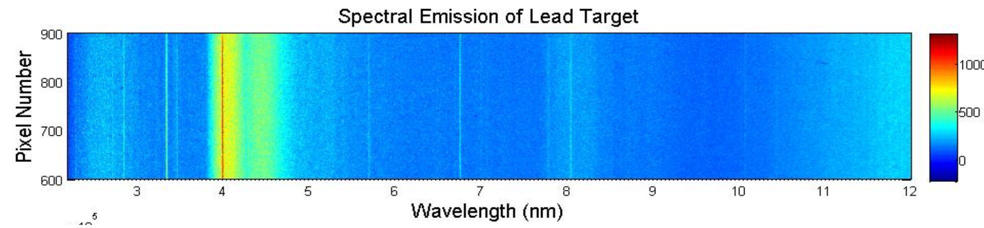

Spectrum consists of:

- lines (bound-bound transitions), in some cases lines cluster together to form a UTA (unresolved transition array)
- recombination radiation (bound-free transitions): $I\ \alpha\ n_e^2\langle z\rangle^4$ where $\langle z\rangle$ is the average ionic charge
- bremsstrahlung (free-free): $I\ \alpha\ n_e^2$,

Maximise line emission by reducing opacity, Maximise spectral purity by reducing recombination

Density has a 'sweet spot'

Most important isoelectronic sequences for line emission

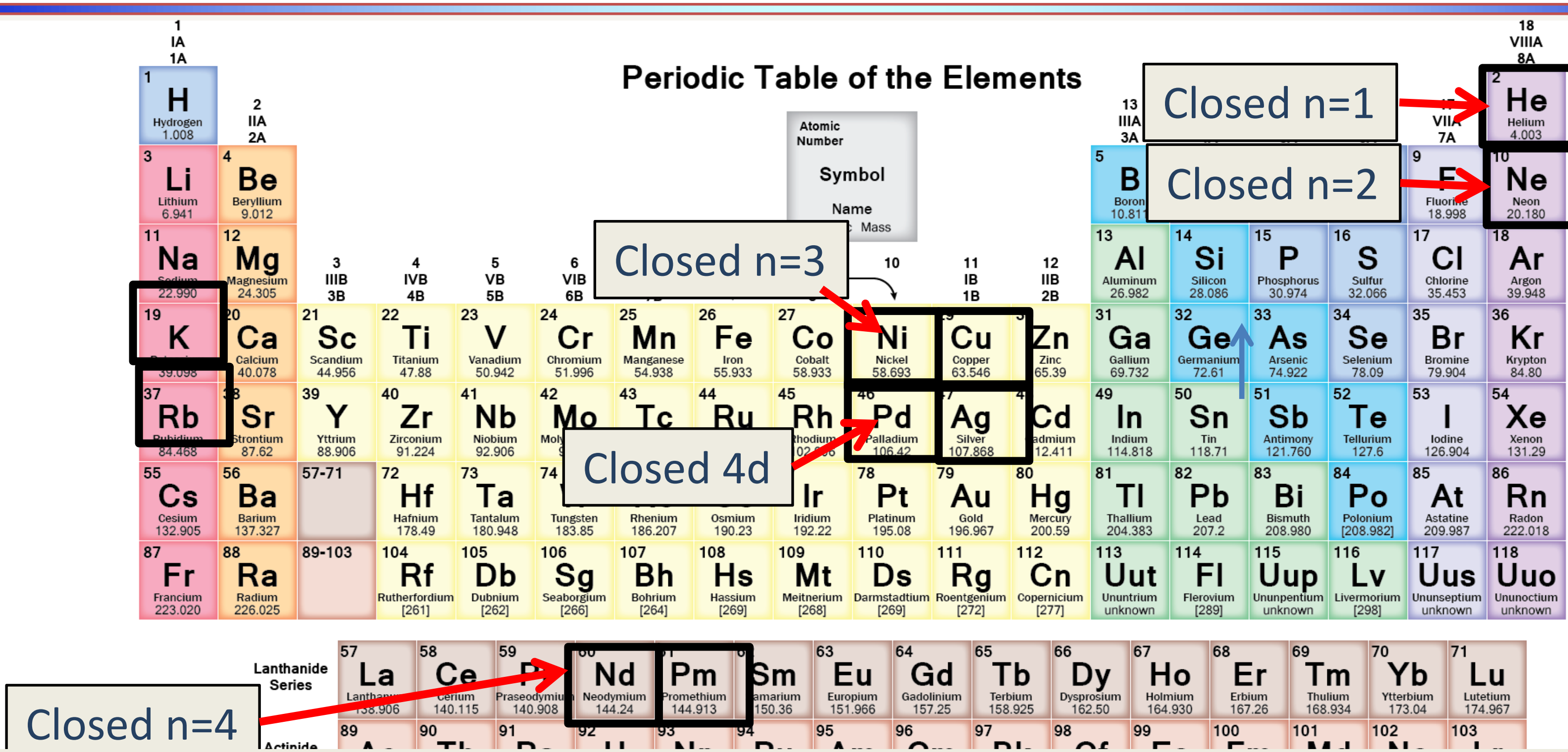

Because of increase in ionization potential required to remove an electron from a closed shell, get large populations of closed shell and single electron outside closed shell species. **Strongest lines from closed shell or single electron outside closed shell species.** Also in LPPs spectra often dominated by these species (especially at short pulse lengths). because of high density, lines from high n states are usually not seen. **Strongest lines always involve resonance transitions to the ground configuration**
Must allow for level rearrangement with ionization.

Subshell ordering with increasing ionization

Ground configurations can change along isoelectronic sequences, levels reorder by principal quantum number.

- In Ca I ground configuration is (Ar) $4s^2$, this changes to (Ar) $3d^2$.
- Hyperalkali ions: PmI: $4d^{10}5s^25p^66s^24f^5$ changes to $4d^{10}\,4f^{14}5s$ at the 15^{th} ion stage along the sequence *(Curtis and Ellis PRL 45, 2099 1989).*
- Xe sequence: transitions based on $5p^6$ vanish at Pr VI, ground configuration changes to $\{5p4f\}^6$.

Reason:

The effective radial potential is of the form:

$$-Z'e^2/4\pi\varepsilon_0 r + l(l+1)h^2/8\pi^2 r^2$$

in neutrals and low ion stages the centrifugal term dominates and causes irregularities in filling of subshells. With increasing ionisation the Coulomb term becomes dominant…………H-like structure

Early studies @13.5 nm, line emission CE

APPLIED PHYSICS LETTERS **93**, 091502 (2008)

Laser wavelength dependence of extreme ultraviolet light and particle emissions from laser-produced lithium plasmas

Akihisa Nagano,[a)] Takayasu Mochizuki, Shuji Miyamoto, and Sho Amano
Laboratory of Advanced Science and Technology for Industry, University of Hyogo, 3-1-2, Kouto, Kamigori, Ako-gun, Hyogo 678-1205, Japan

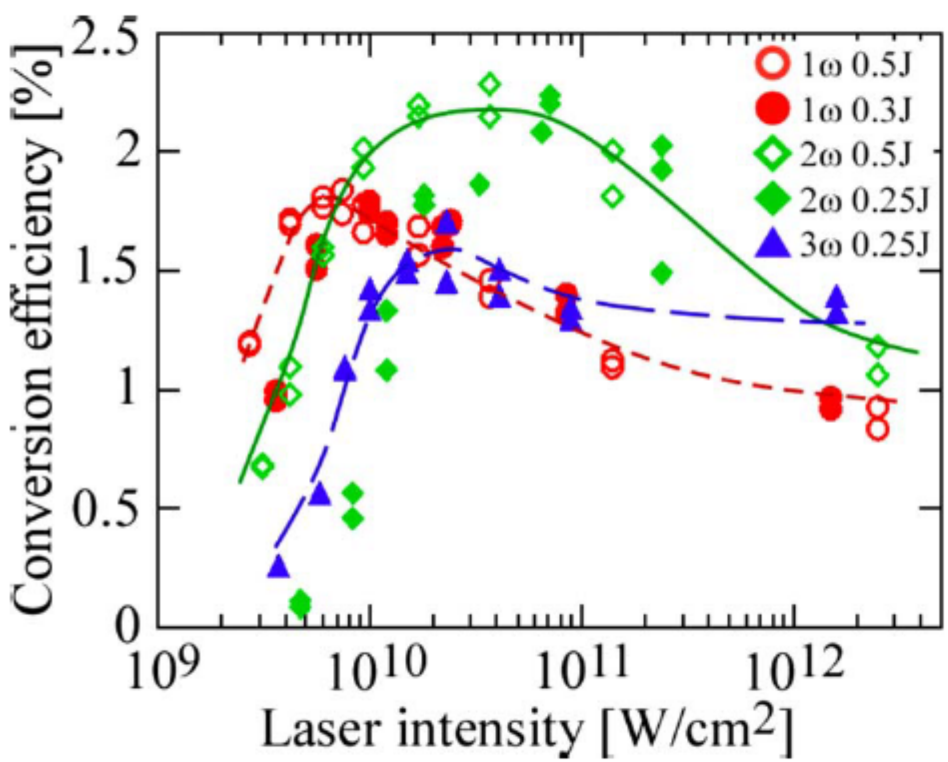

Line Source:
Li: 1s-2p transition at 13.5 nm

Conversion efficiency (CE)
~ 2.3% @ λ = 532 nm,
~ 1.8% @ λ = 1064 nm

Up to 4% using forced recombination predicted.

Spot size ~400µm, τ = 10 ns
CE dropped at small spot sizes due to lateral expansion

More ablation at λ = 532 nm,
Opacity reduced output at 355 nm

Two types of UTA in XUV spectra

Δn = 0

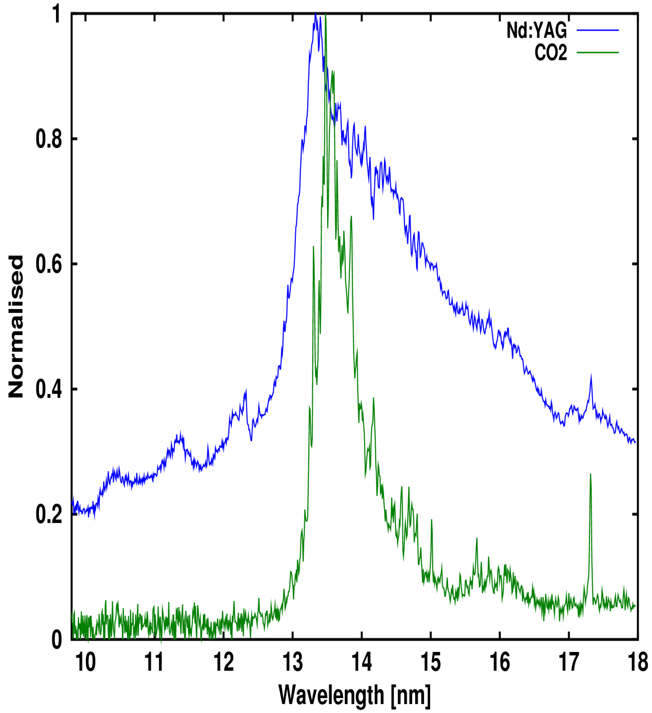

$4p^6 4d^N$- $4p^6 4d^{N-1} 4f + 4p^5 4d^{N+1}$ in Sn @13.5 nm, emission from different ion stages overlap. Opacity is a major issue.

Δn > 0

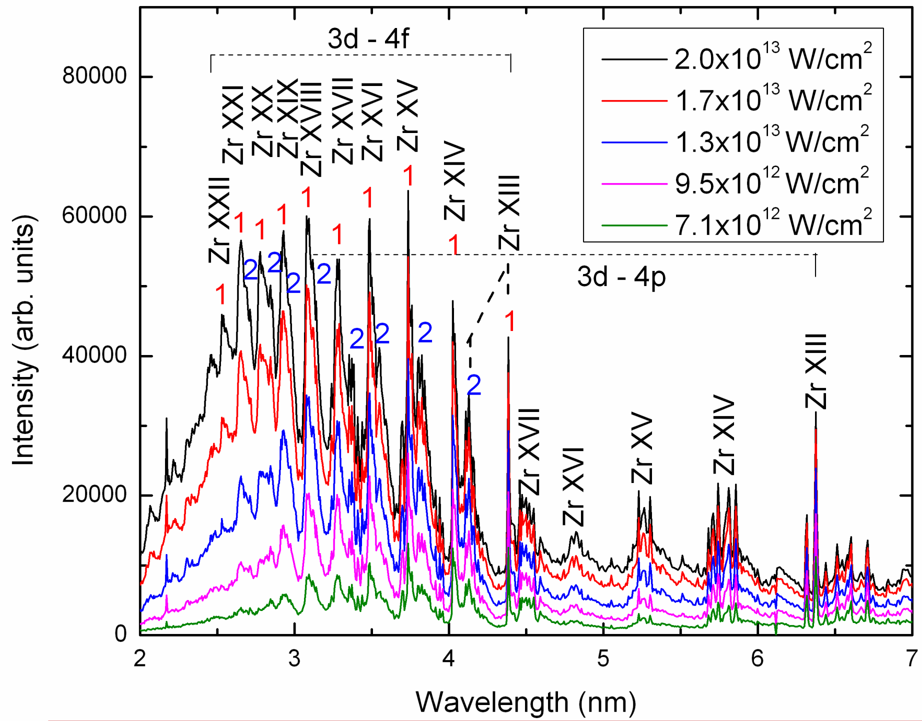

Δn = 0 transitions overlap in adjacent ion stages.

Δn > 0 transitions do not overlap in adjacent ion stages and move to shorter wavelengths with increasing ionization….less opacity.

Outline

- Applications of Laser Produced Plasmas (LPPs) as Light Sources for Lithography and Microscopy.
- Properties of LPPs
- Properties of $\Delta n = 0$ UTAs
- Application of $\Delta n = 1$ UTAs
- Conclusions

Δn = 0 UTA: important isoelectronic sequences

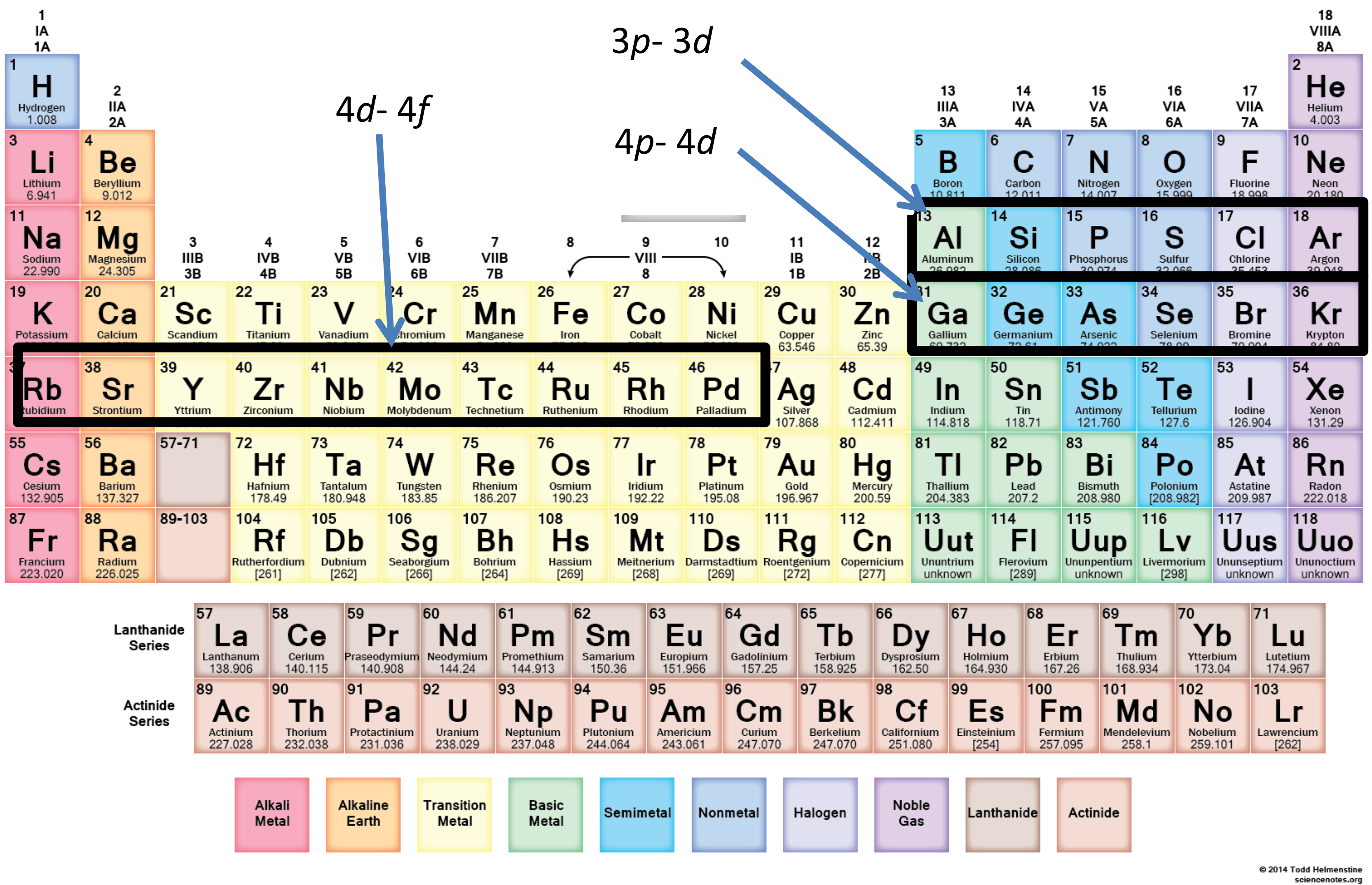

$4p$-$4d$ $\Delta n = 0$ UTA

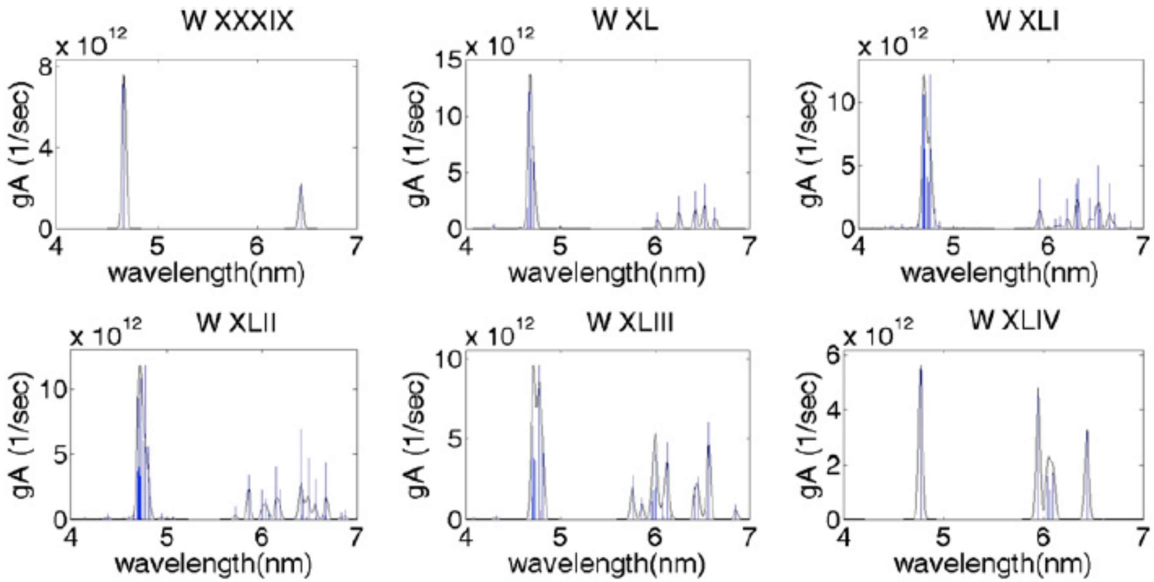

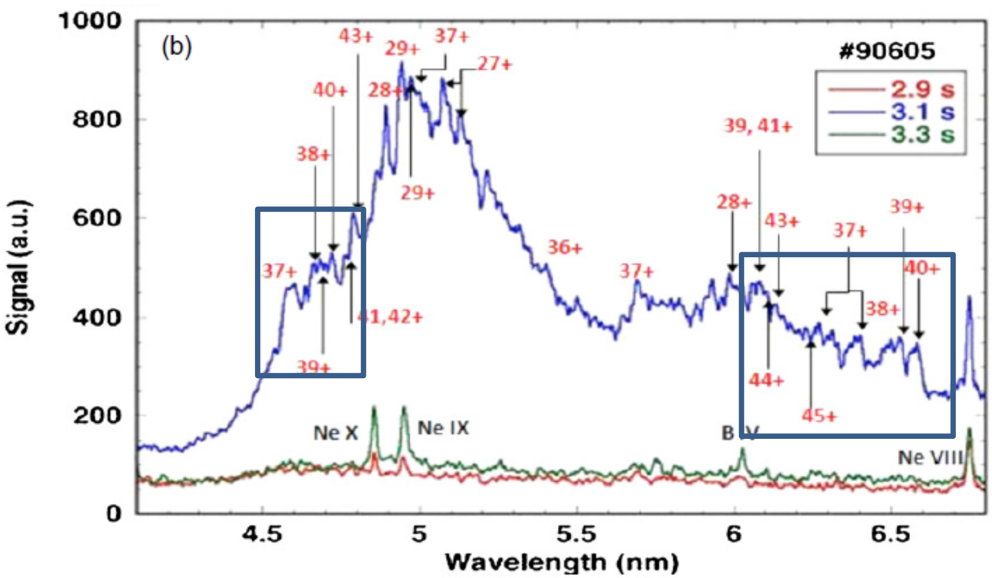

$4p^n$- $4p^{n-1}4d$ UTA, important in lanthanides and 3rd transition row spectra.

Spin orbit split, overall, relatively weak and high energy array lies on the short wavelength side of the 5 nm UTA in W.

Sn UTA emission

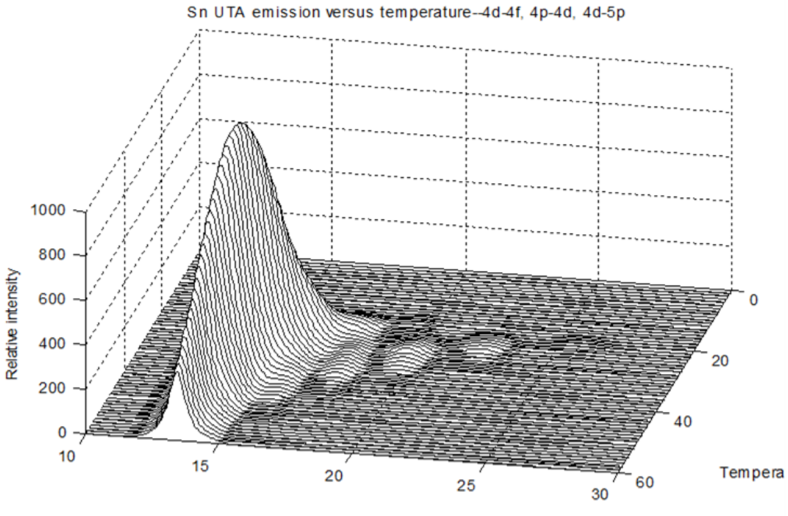

$4p^6 4d^N$- $4p^6 4d^{N-1} 4f$ emission in Sn @13.5 nm

Increasing power density ↓

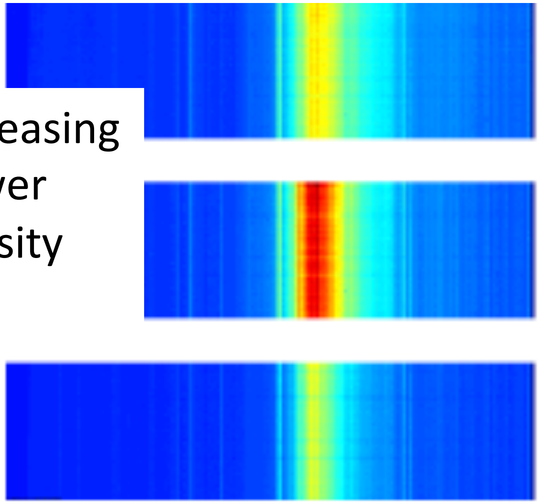

Lines due to SnXI –Sn XIV

Churilov and Ryabtsev, 2006,Phys. Scr. 73 614-619

More recent study has shown the need to revisit and refine analysis

Windberger et al. 2016, PRA 94, 012506 Toretti et al PRA 95 042303 2017

Major problem due to spectral complexity

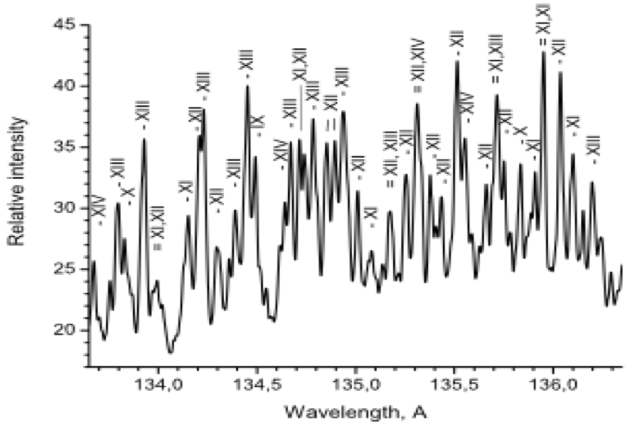

Spectral shape modified by density effects: opacity, satellite lines

Sasaki et al. 2004. IEEE Journal of Quant. Electron.10, 1307

Evolution with Z of Δn=0, 4d-4f UTAs

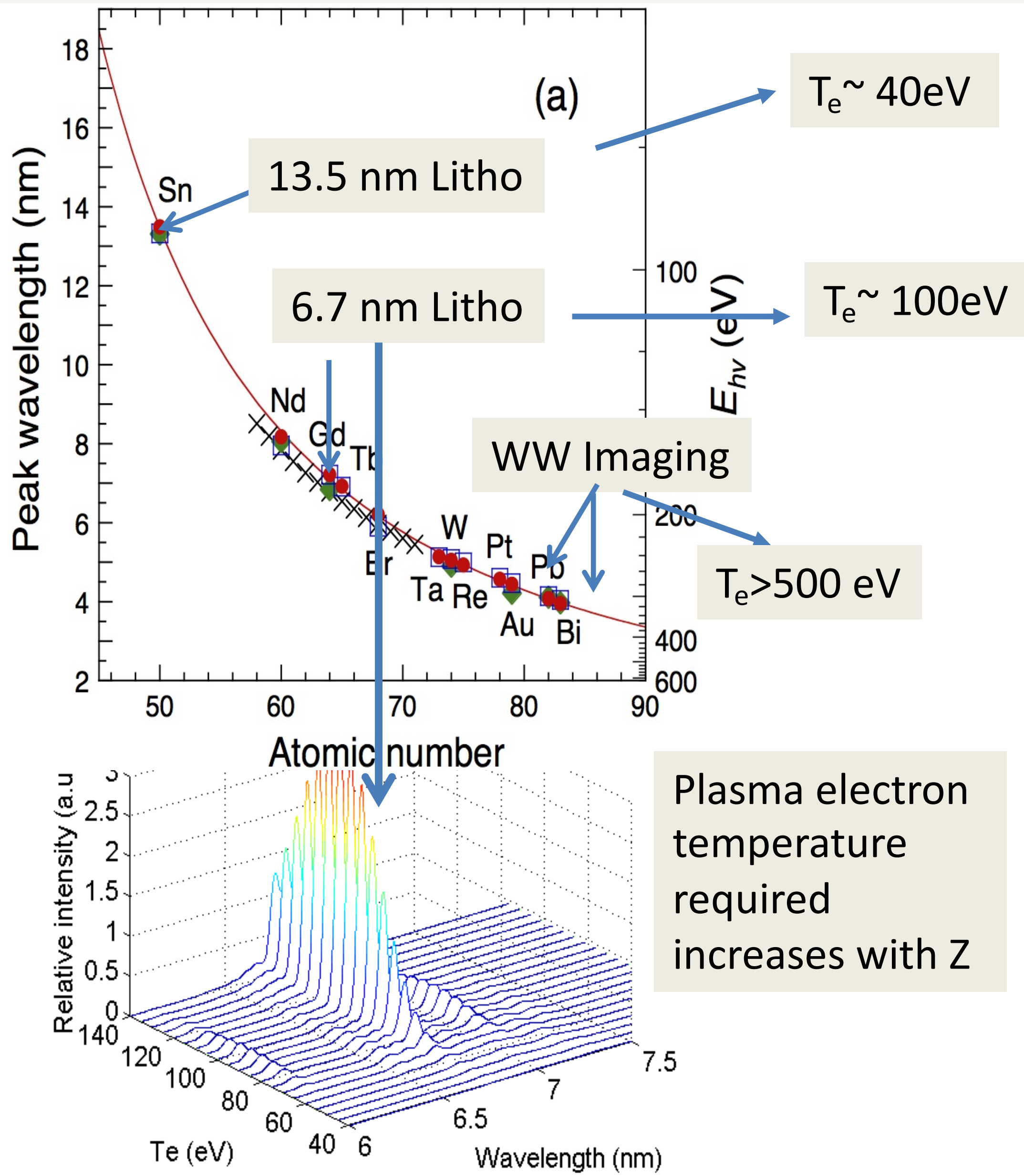

Plasma electron temperature required increases with Z

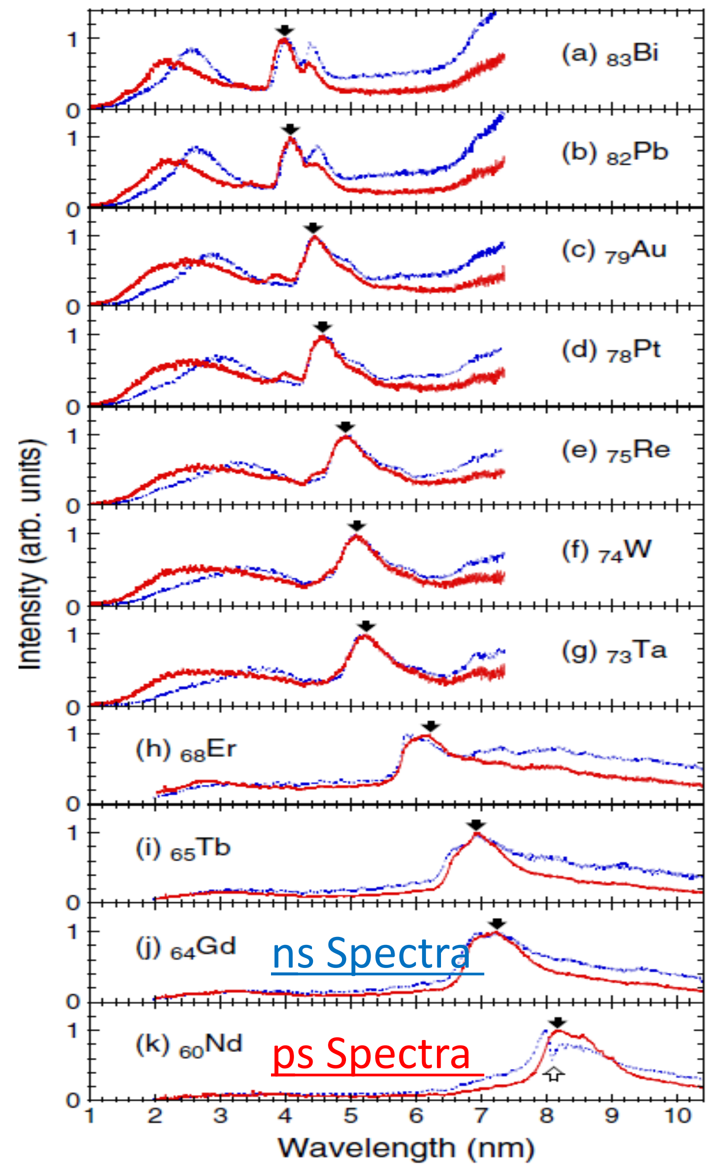

Spectral narrowing due to Configuration Interaction

For $4p^6 4d^{N+1}$- $4p^6 4d^N 4f$ + $4p^5 4d^{N+2}$ configuration interaction (CI) causes

- Spectral narrowing.
- Strong peaking of oscillator strength.

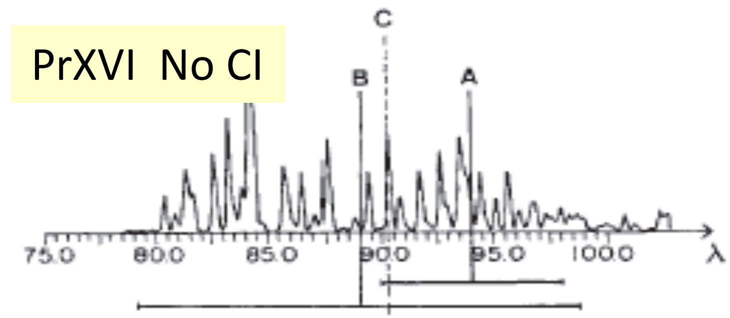

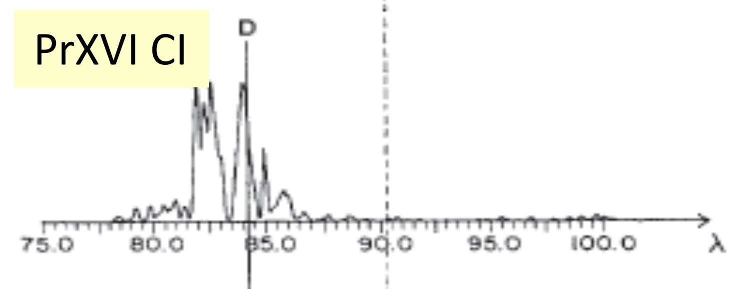

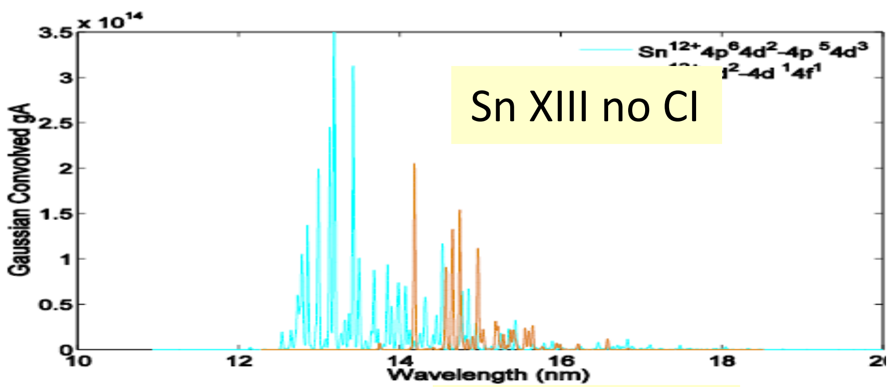

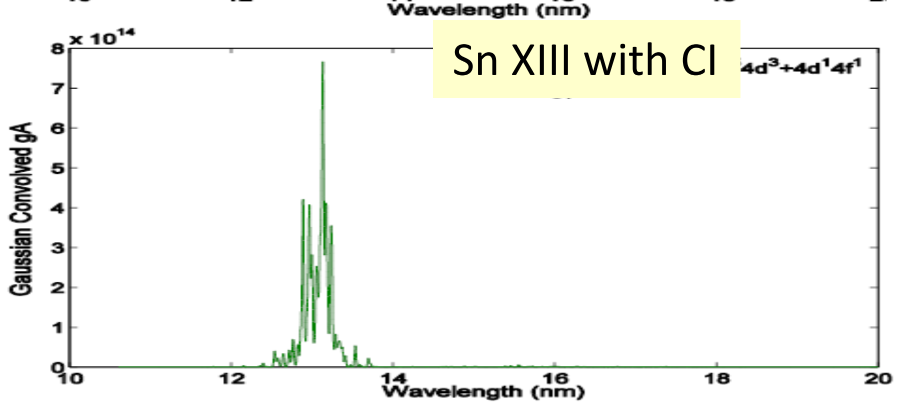

(Mandelbaum et al. PRA 35, 5051 (1987) , Bauche et al. Phys. Scr. 37, 359, 1988)

Spectral narrowing greatly enhances UTA intensity

5*d*-5*f* UTA weaker as CI effects are less important.

Need to isolate the contribution from each ion stage

Use ECR or EBIT Source

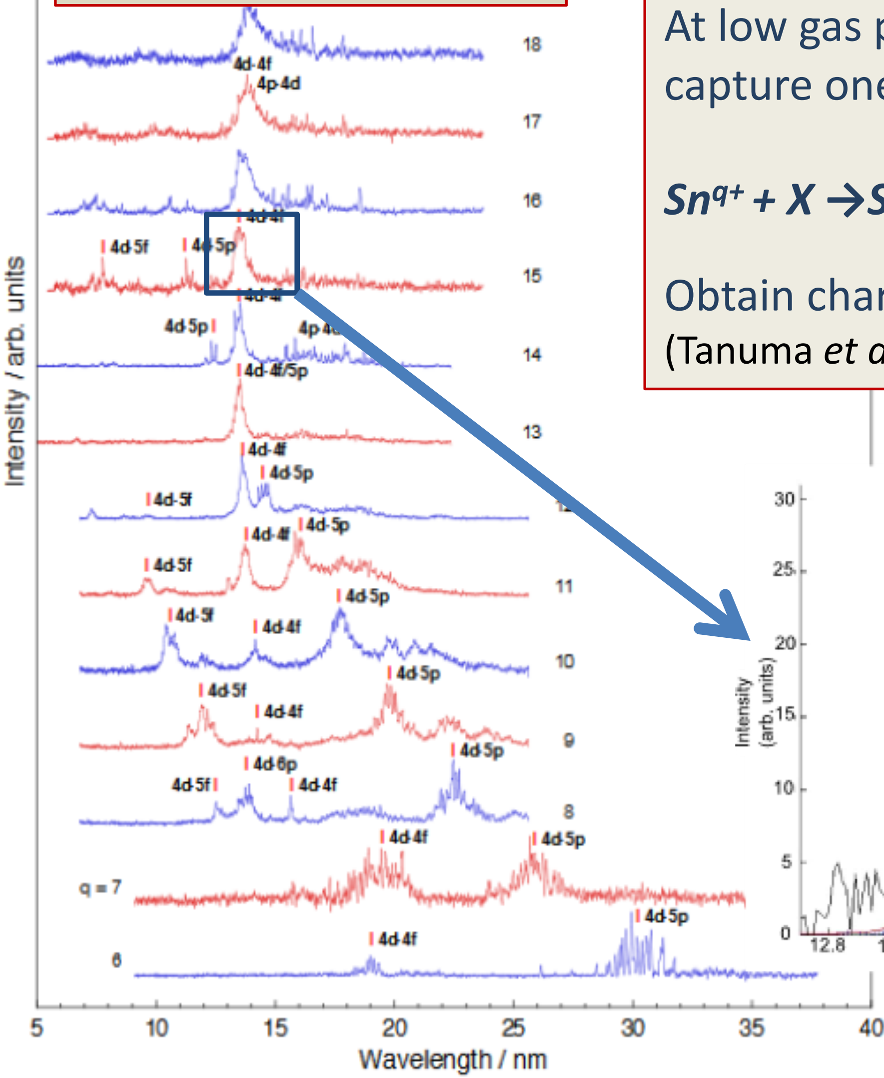

ECR Source Spectra

At low gas pressure in target chamber, Sn ions from ECR capture one electron.

$$Sn^{q+} + X \rightarrow Sn^{(q-1)+*} + X^{+}$$

Obtain charge state selected spectra

(Tanuma *et al*. J. Phys Conf . Series 58, 231, 2007)

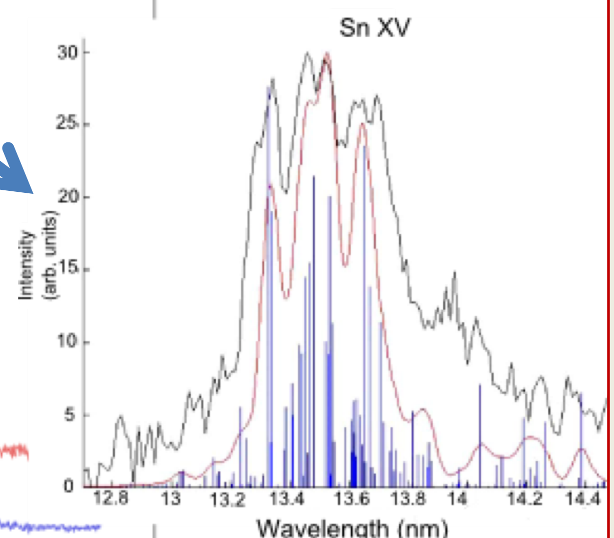

In Sn XV, ground state is $4p^6$, expect $4p - 4d$ $^1S_0$ - $^1P_1$ transition, one strong line.

Observe a UTA, due to excited to excited state ($4d - 4f$) transitions

CX spectra dominated by satellite emission

*(D'Arcy et al. PRA **79**, 042509, 2009)*

EBIT (Electron Beam Ion Trap) Spectra

PHYSICAL REVIEW A **95**, 042503 (2017)

Optical spectroscopy of complex open-4*d*-shell ions Sn^{7+}–Sn^{10+}

F. Torretti,[1,2,*] A. Windberger,[1,3] A. Ryabtsev,[4,5] S. Dobrodey,[3] H. Bekker,[3] W. Ubachs,[1,2] R. Hoekstra,[1,6] E. V. Kahl,[7] J. C. Berengut,[7] J. R. Crespo López-Urrutia,[3] and O. O. Versolato[1]

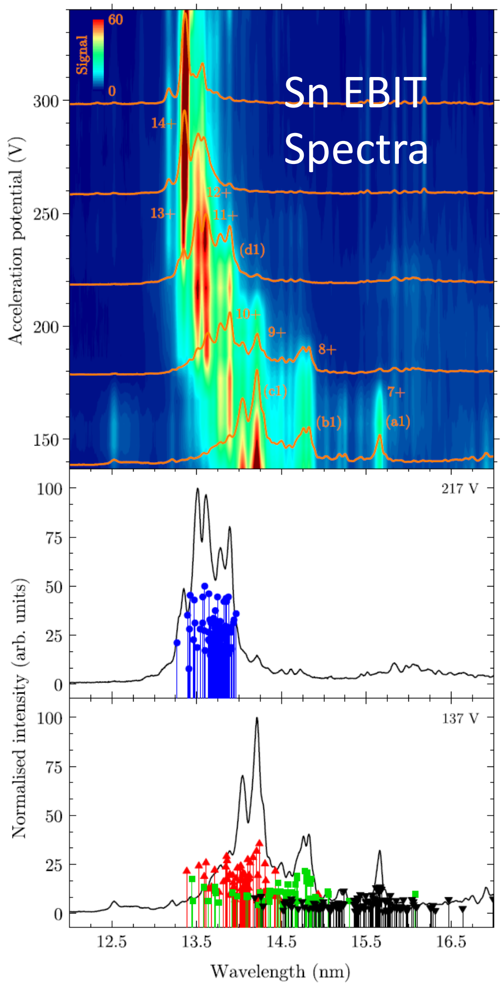

EBIT spectra at higher electron accelerating voltages give spectra from higher ion stages, However, they are generally very weak and recorded at low resolution. Good for strongest lines.

Need for high resolution LPP or vacuum spark spectra in tandem with

low resolution EBIT data for a complete analysis.

Gd EBIT Spectra

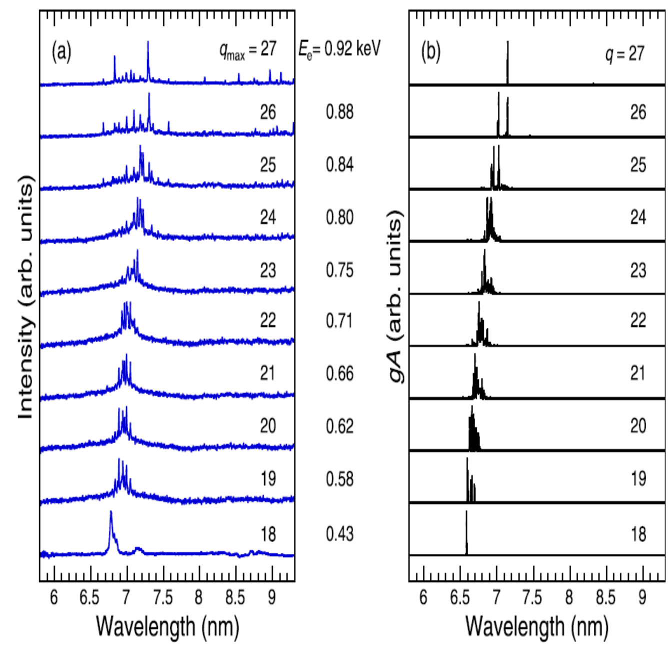

JOURNAL OF APPLIED PHYSICS **115**, 033302 (2014)

Tuning extreme ultraviolet emission for optimum coupling with multilayer mirrors for future lithography through control of ionic charge states

Hayato Ohashi,[1,a)] Takeshi Higashiguchi,[1,b)] Bowen Li,[2] Yuhei Suzuki,[1] Masato Kawasaki,[1] Tatsuhiko Kanehara,[3] Yuya Aida,[3] Shuichi Torii,[4] Tetsuya Makimura,[4] Weihua Jiang,[5] Padraig Dunne,[2] Gerry O'Sullivan,[2] and Nobuyuki Nakamura[3]

Opacity Effects in Δn = 0 n=4-n=4 arrays

- Spectra from metal targets dominated by continuum emission

  Some strong emission and absorption lines

  Large **contribution from satellite lines**

- Spectra of low density targets dominated by an intense Unresolved Transition Array (UTA), with greatly reduced continuum emission

  Emission largely mirrors line strength distribution

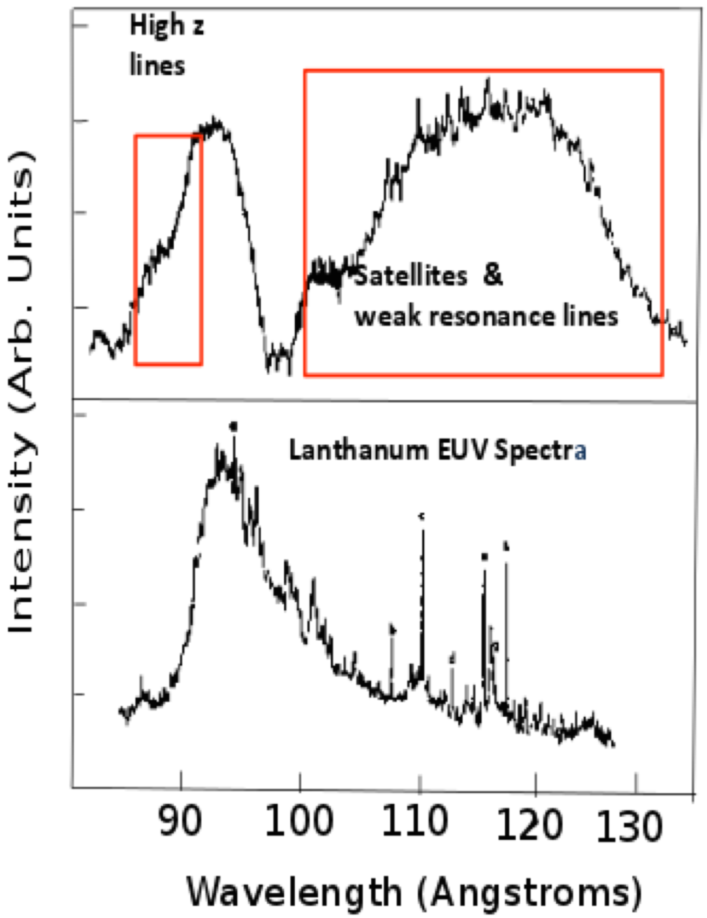

Narrowing of the UTA at reduced ion concentration

Dominant emission in all ion stages arises from $4p^6 4d^N$ - $4p^6 4d^{N-1} 4f + 4p^5 4d^{N+1}$

Emission from $4d^{N-1}nf$ (n>4) are reduced in intensity

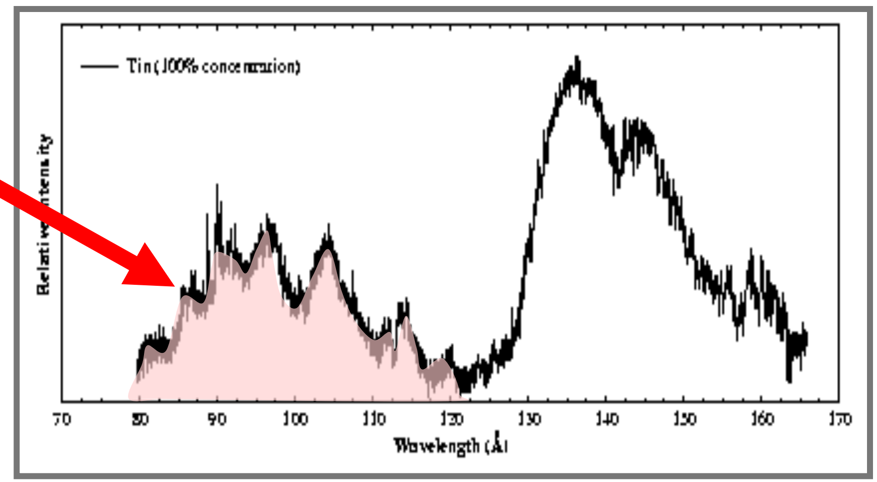

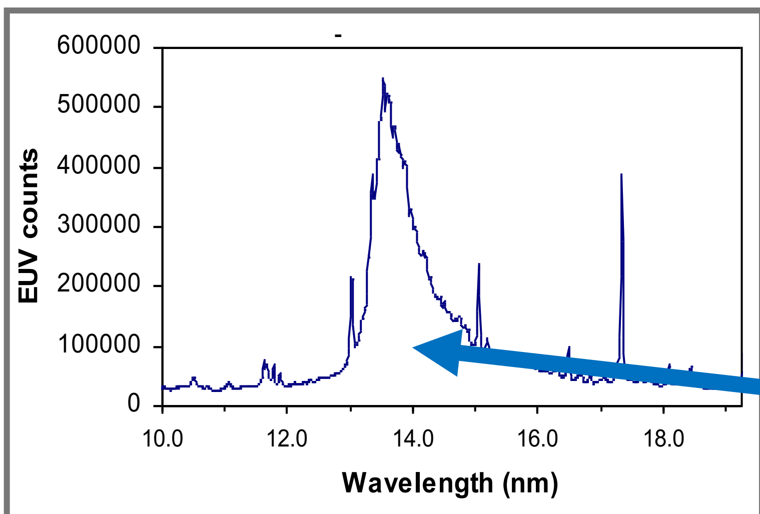

UTA at ~ 13.5 nm now appears narrower and is less affected by absorption

LHD spectra of Sn

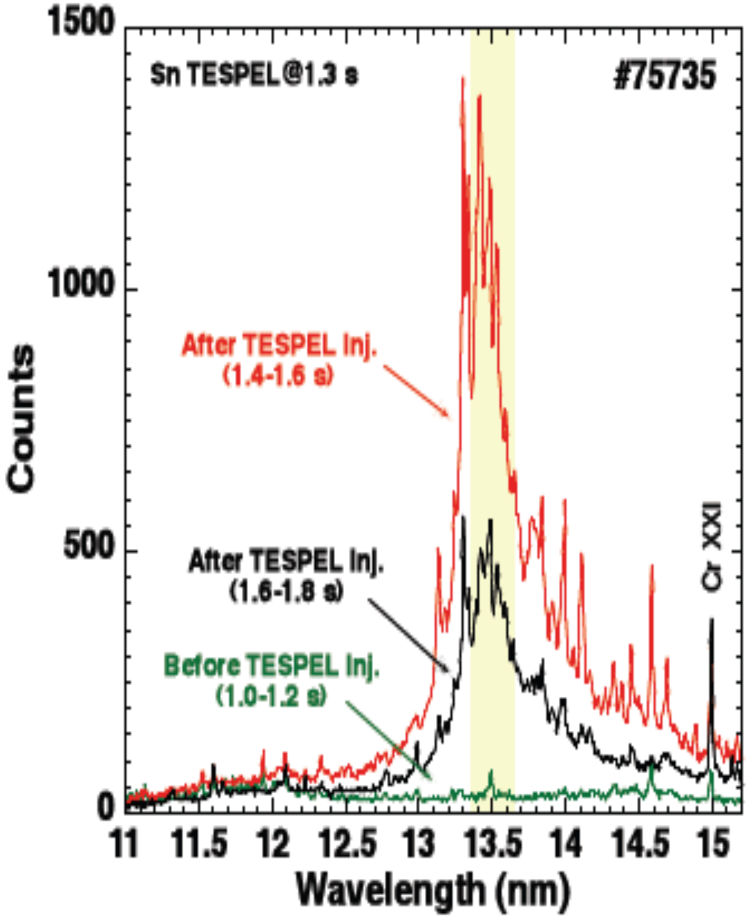

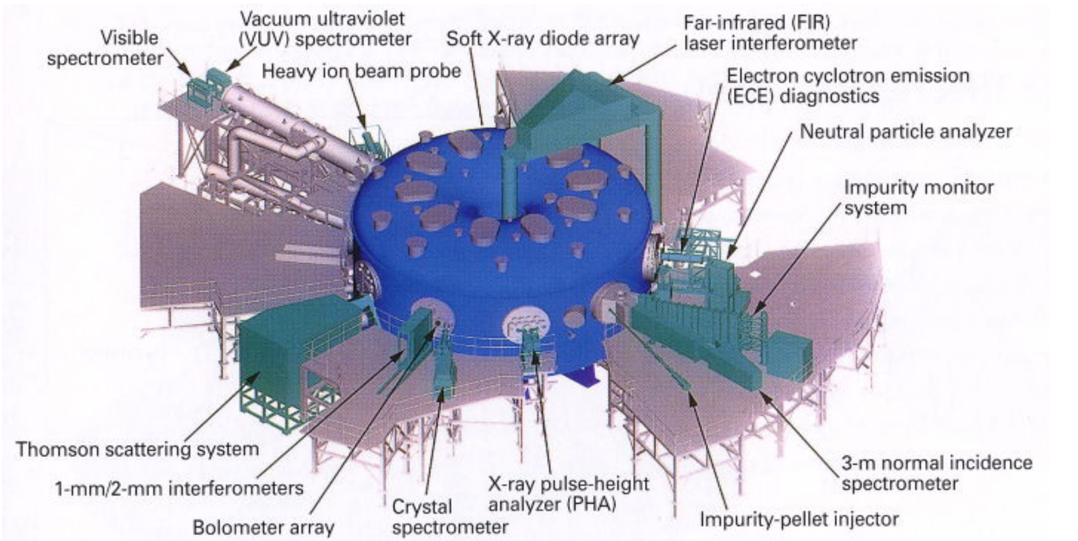

- Sn injected using a TESPEL.
- Spectra dominated by resonant line emission to the ground state
- Absorption free, emission mirrors gA-values

(Suzuki et al JPB 4 , 074027, 2010)

Effect of Laser Wavelength: CO_2 *vs.* Nd:YAG

1-D Hydro modeling – demonstrated increase in CE for CO_2

CE for CO_2 ~ 2x Nd:YAG value.
*J. White et al, Appl. Phys. Lett., **90**, 181502 (2007)*

Temperature depends on laser power density (Φ).

$$T_e(\mathrm{eV}) \approx (\lambda^2\Phi)^{3/5}$$

Average charge $\approx 0.67\,(AT_e)^{1/3}$

$n_{ec} \approx 10^{21}\lambda^{-2}$ (cm^{-3})

1,064 nm: $n_{ec} \approx 1\times10^{21}\ \mathrm{cm}^{-3}$
10,600 nm: $n_{ec} \approx 1\times10^{19}\ \mathrm{cm}^{-3}$

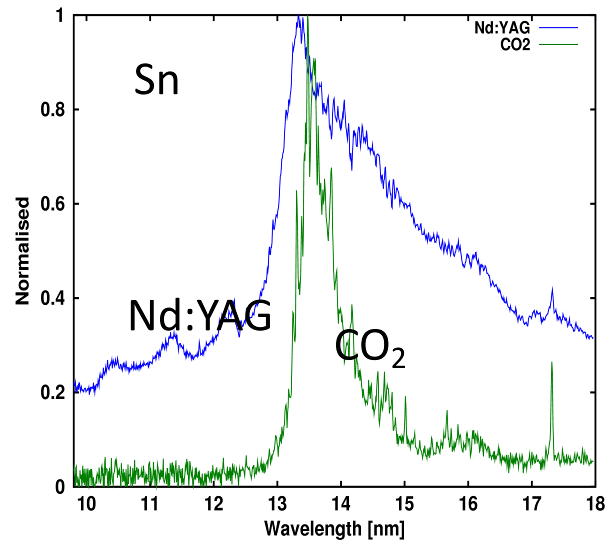

- **Less energy, better CE**
- **Improved opacity**
- **Lower power density required**

Optical depth α pulse duration$\times$(Intensity)$^{5/9}$ $\times(\lambda)^{-4/3}$

Increases with pulse duration, decreases with laser wavelength.
.(Ando *et al. APL* ***89****, 151501, 2006, Sunahara et al Plasma and Fusion Res.3,43 2008)*

Effect of prepulses with slab targets

Single Pulse Spectrum

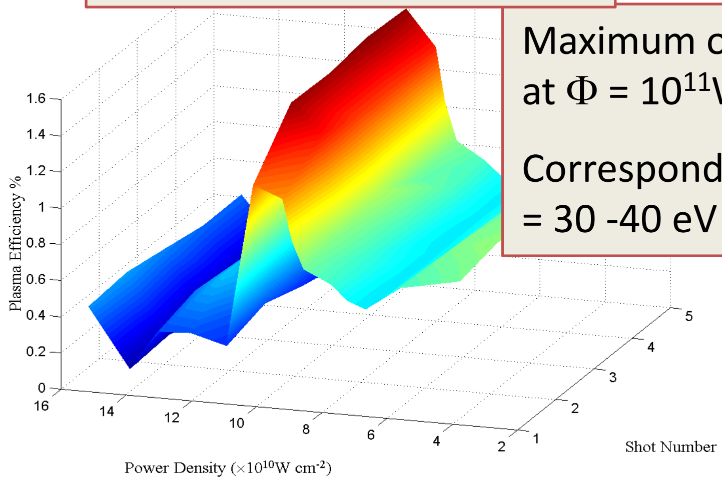

Maximum output at $\Phi = 10^{11}$Wcm^{-2}.

Corresponding Te = 30 -40 eV

The use of prepulses greatly enhances intensity in X-ray and EUV regimes
e. g. Mochizuki et al. 1986 PRA33, 525,Kodama et al. 1987APL. 50, 720. Tanaka et al. 1988JAP . 63, 1767, Teubner et al. 1991,APL. 59,2672, Wulker et al. PRE 1994, 4920

Efficiency increases due to increased emitting volume with lower density and opacity (equivalent to using a CO_2 laser.)

Sn output (≈`5% bw) at 13.5 nm as a function of delay & %.

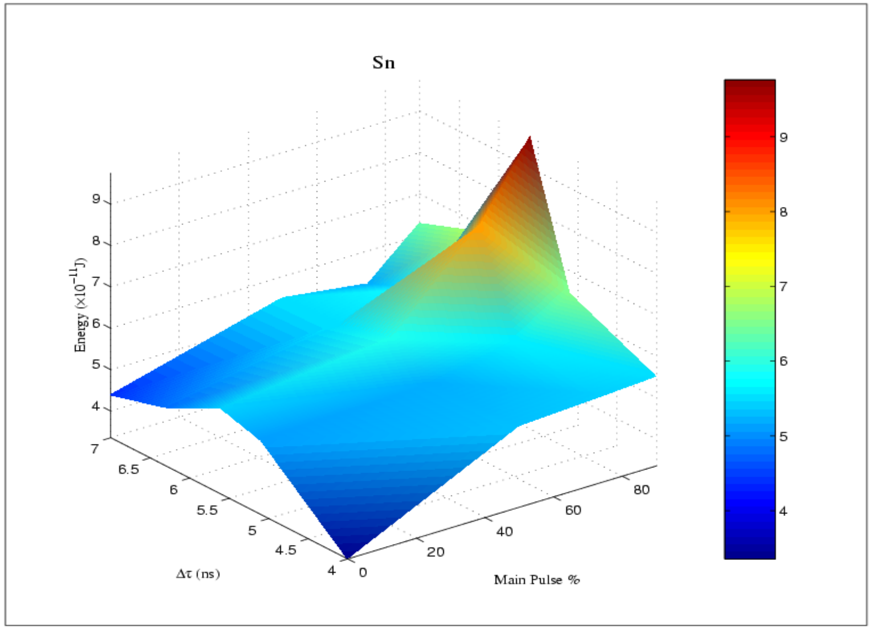

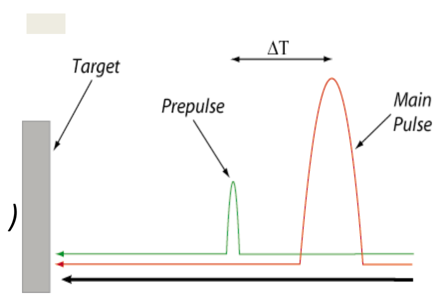

Optimum ratio: 10/90,
Optimum $\Delta\tau$ = 5.5 ns

Gain ~ 80%
Pulse: λ = 1064 nm,
$\Delta\tau$ = 170 ps
$\Phi = 3\times10^{12}$ Wcm^{-2}

What is Max CE?

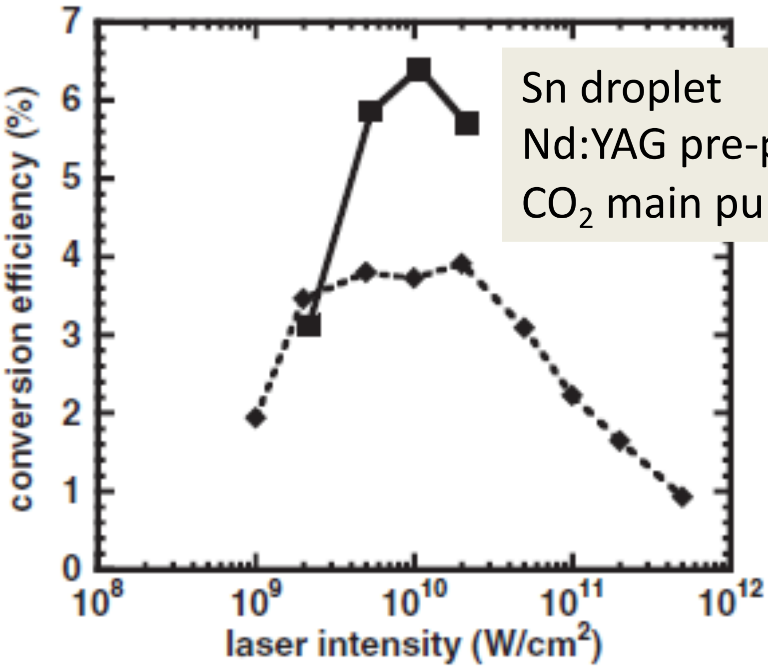

Sn droplet
Nd:YAG pre-puls
CO_2 main pulse

Conversion efficiency dependence on CO_2 laser intensity for single (dashed) and double (solid) irradiation by a 10 ns pulse. The interpulse delay was 180 ns *(Nishihara et al Phys. Plasmas 15, 056708 2008)*

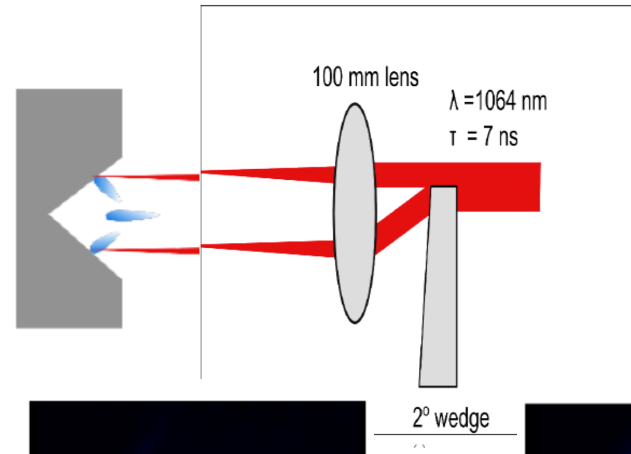

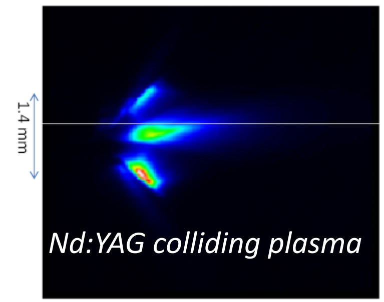

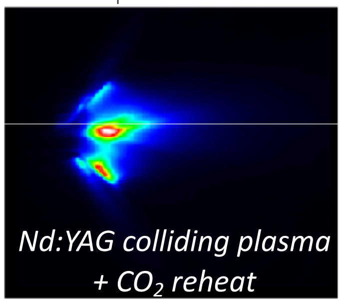

Max CE @ 60 ns delay close to wedge centre

Nd:YAG, E~ 170 mJ, $\Phi = 1.5\text{x}10^{11}$ Wcm^{-2}

CO_2: E~ 200 mJ, $\Phi = 4\text{x}10^9$ Wcm^{-2}

CE = 3.33±0.16%

For CO_2 only, CE = 4.85±0.10%

Allowing for overfilling of plasma by CO_2

CE approximately 7%

4d-4f UTA at shorter wavelengths: 6.x nm

Optimum temperature for an optically thin Gd plasma ~110 eV
Maximum intensity at 6.76 nm due to $4d^{10}\,{}^1S_0$- $4d^9 4f\,{}^1P_1$ line.

Hybrid UTA-line source

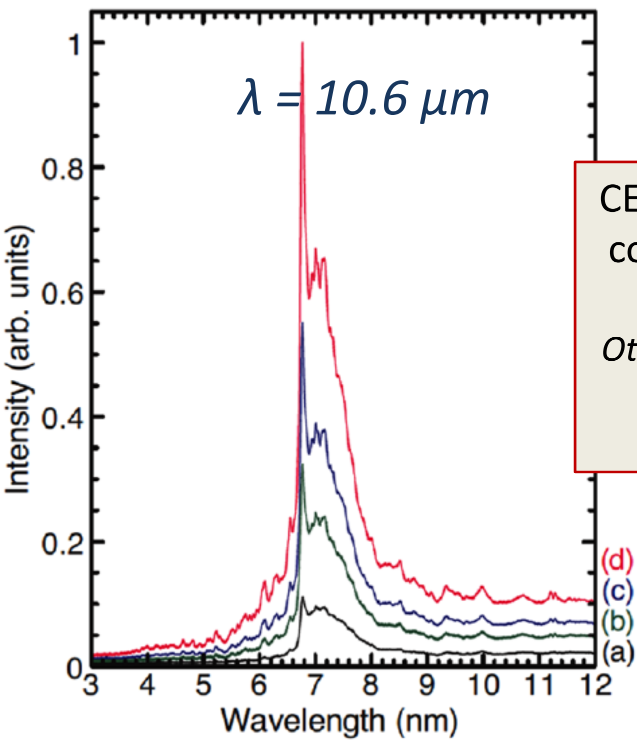

CE improves as concentration decreases
Otsuka et al. APL 97, 111503 (2010)

IOP Publishing — Physica Scripta
Phys. Scr. 80 (2009) 045303 (6pp) — doi:10.1088/0031-8949/80/04/045303

EUV spectra of Gd and Tb ions excited in laser-produced and vacuum spark plasmas

S S Churilov[1], R R Kildiyarova, A N Ryabtsev and S V Sadovsky
Establishment of the Russian Academy of Sciences Institute of Spectroscopy RAS, Troitsk, Moscow region 142190, Russia

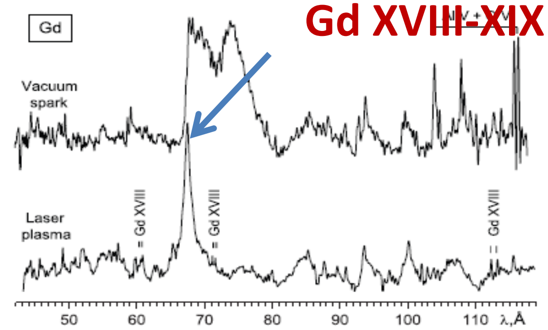

Gd XVIII-XIX

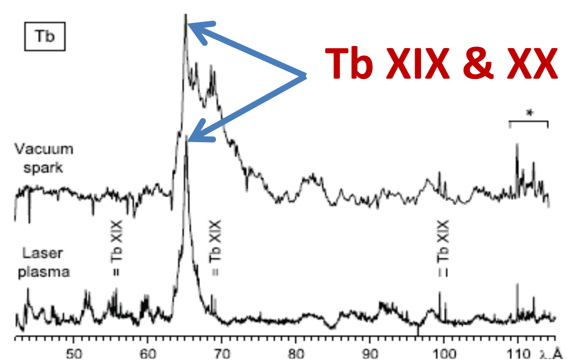

Tb XIX & XX

3 J in 20 ns, λ = 1.06 µm
$\Phi = (5–8)\times10^{11}$ Wcm^{-2}

The most important transitions occur in Ag-like and Pd-like:
Gd XVIII-XIX, Tb XIX - XX

i.e. Ions with $4d^{10}4f$ and $4d^{10}$ and ground states

(Sugar and Kaufman Phys. Scr. ***24****, 742 (1982) and* ***26****, 417 (1984))*

CE Experiment at Gekko XII

Spherical target

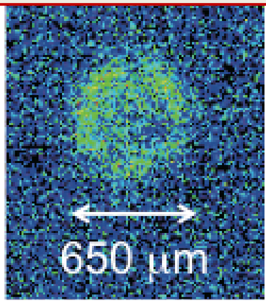

12 beams from Gekko XII, λ=1.053 mm E=1 J, E(Total)=12 J, τ=1.3 ns. Quasi1-D expansion for each beam. *(Yoshida et al Appl. Phys. Exp. 7, 086202 2014)*

CE=0.8%

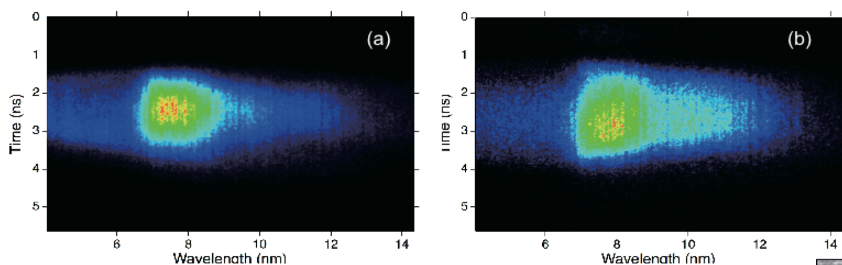

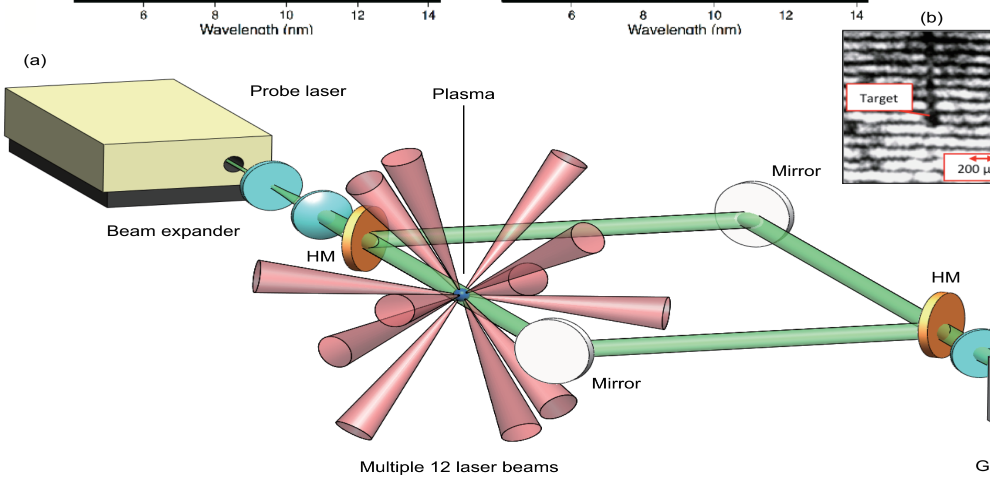

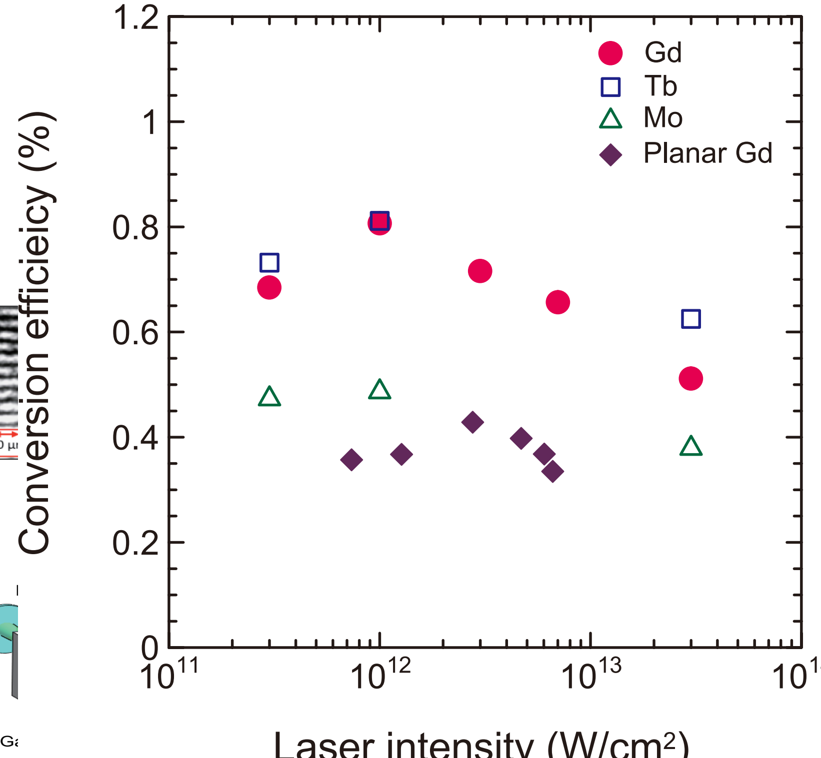

CE lower than Sn as higher fraction of laser energy goes into plasma heating/ionizaton

4p-4d and 4d-4f arrays separate as Z increases

Note that 4d-4f moves to longer wavelength with increasing ionization

$4p^6 4d^{N+1}$- $4p^6 4d^N 4f$

$$\delta E = N\frac{(2l+1)(2l'+1)}{4l+1}\left(\sum_{k\neq 0} f_k F^k(l\,l') + \sum_k g_k G^k(l\,l')\right)$$

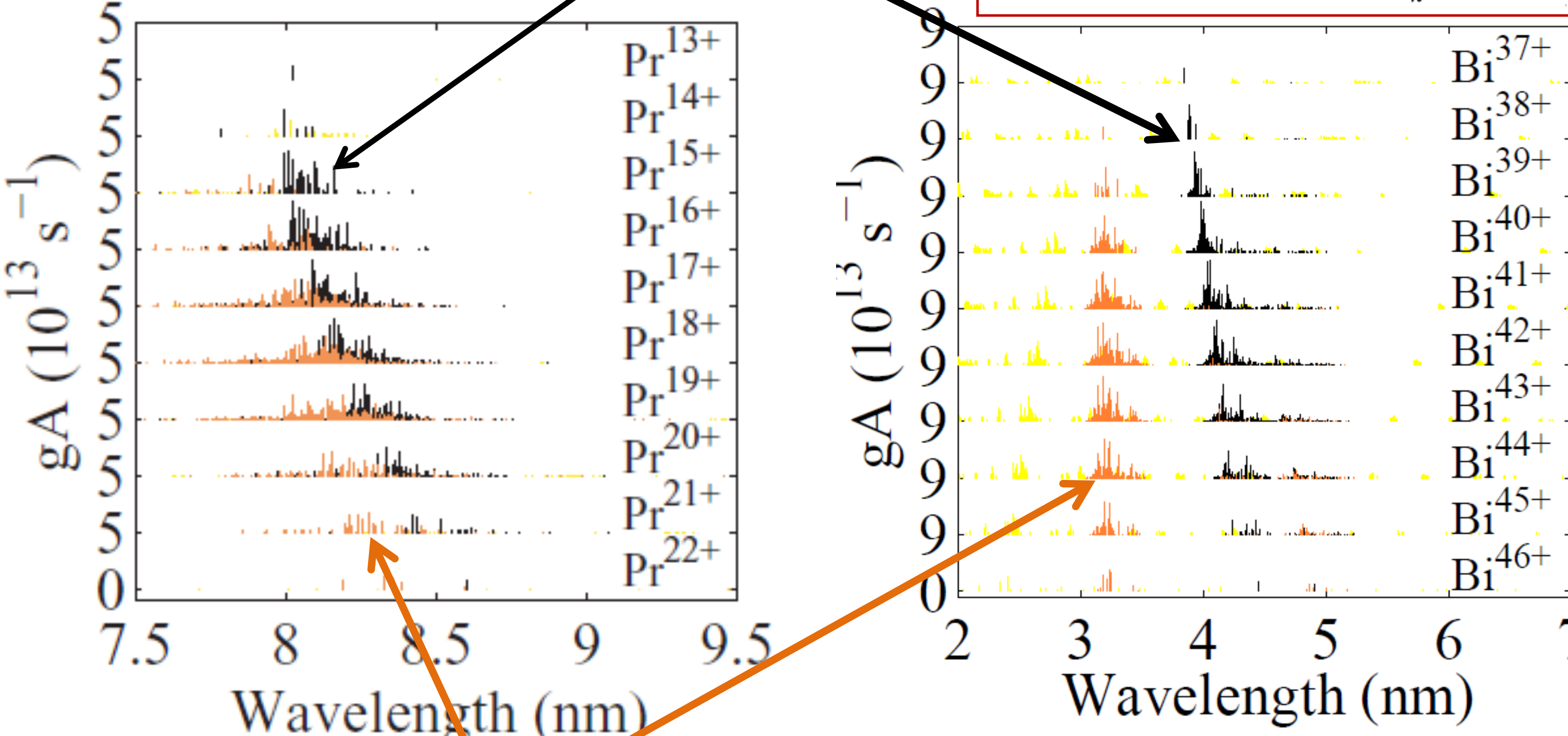

$4p^6 4d^{N+1}$- $4p^5 4d^{N+2}$

Kilbane and O'Sullivan PRA 82, 062504 (2010)
Kilbane JPB 44 165006 (2011)

Intensity Scaling of n= 4 – n=4 UTAs

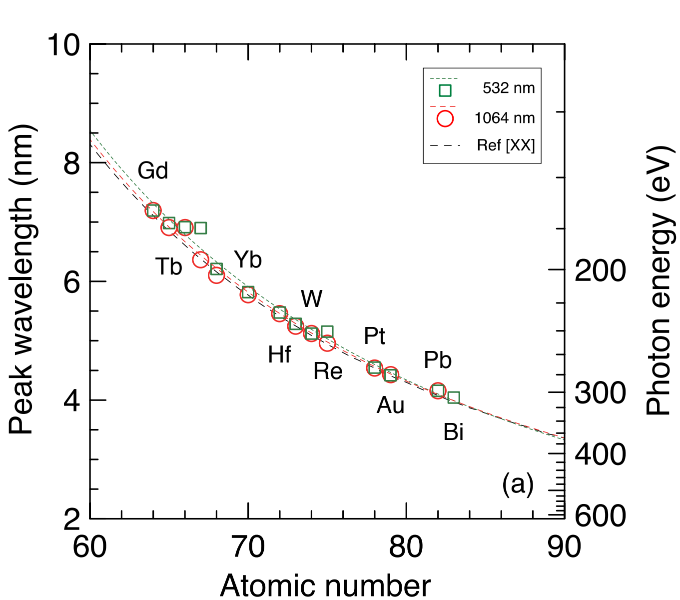

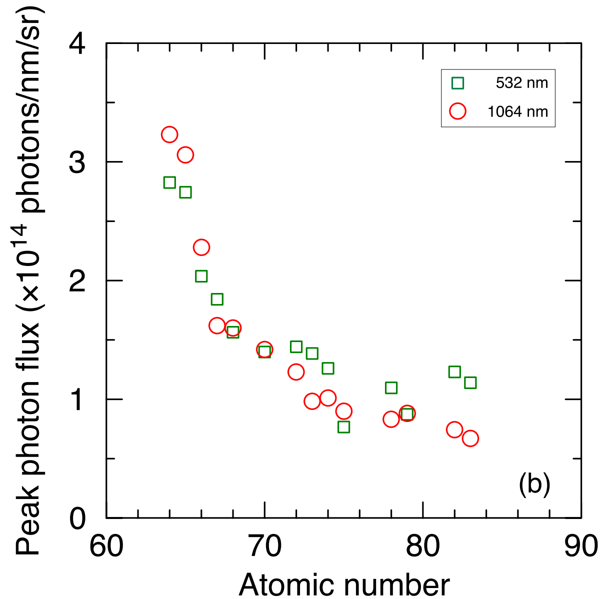

Atomic number dependences of the wavelength and photon flux of the n = 4 – n = 4 (Δn = 0) transitions.
(Shimada et al. APL 2019 Submitted)
Note that intensity falloff past Z = 70 due to decreasing HCI population is compensated for by diminishing impact of absorption due to $4p^6 4d^n \rightarrow 4p^5 4d^{n+1}$ transitions

Δn = 0 4-4 UTAs in the water window region, Au, Pb and Bi (LHD Spectra)

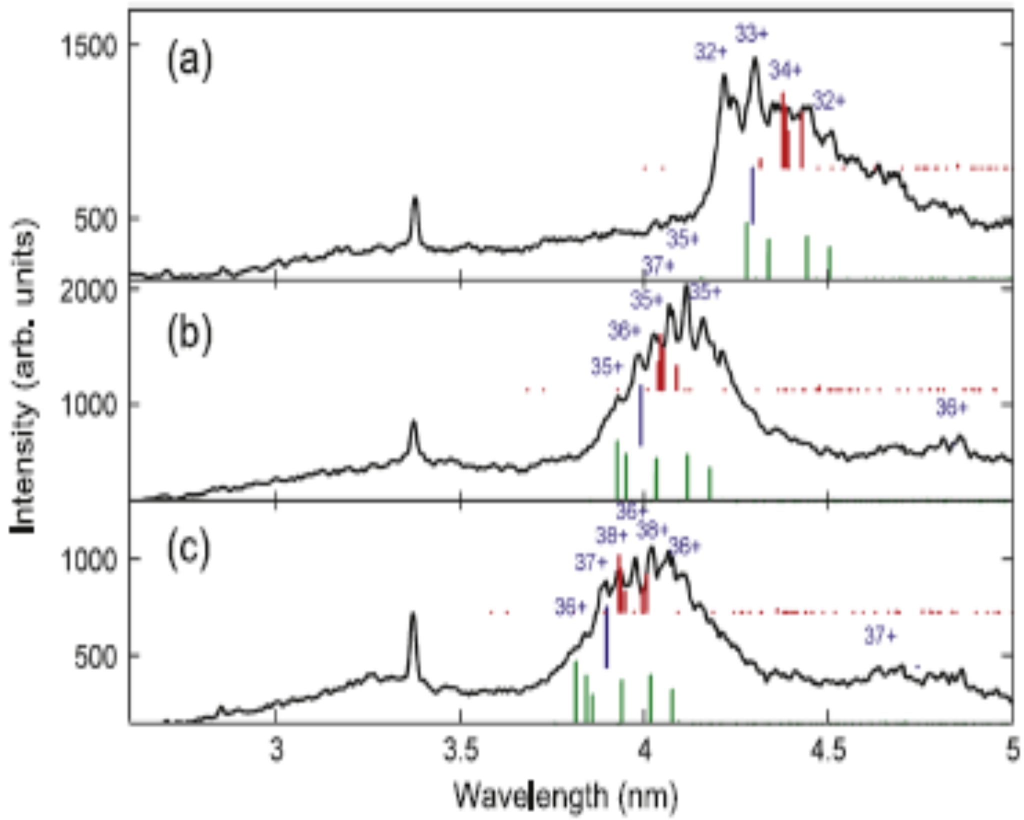

•Spectra dominated by resonant line emission to the ground state

•Only Ag-, Pd- and Rh-like ions give line emission

Absorption free *(Ohashi et al. JPB 48 (2015) 144011)*

All require Te> 500 eV for generation

LPP Spectrum of Pb

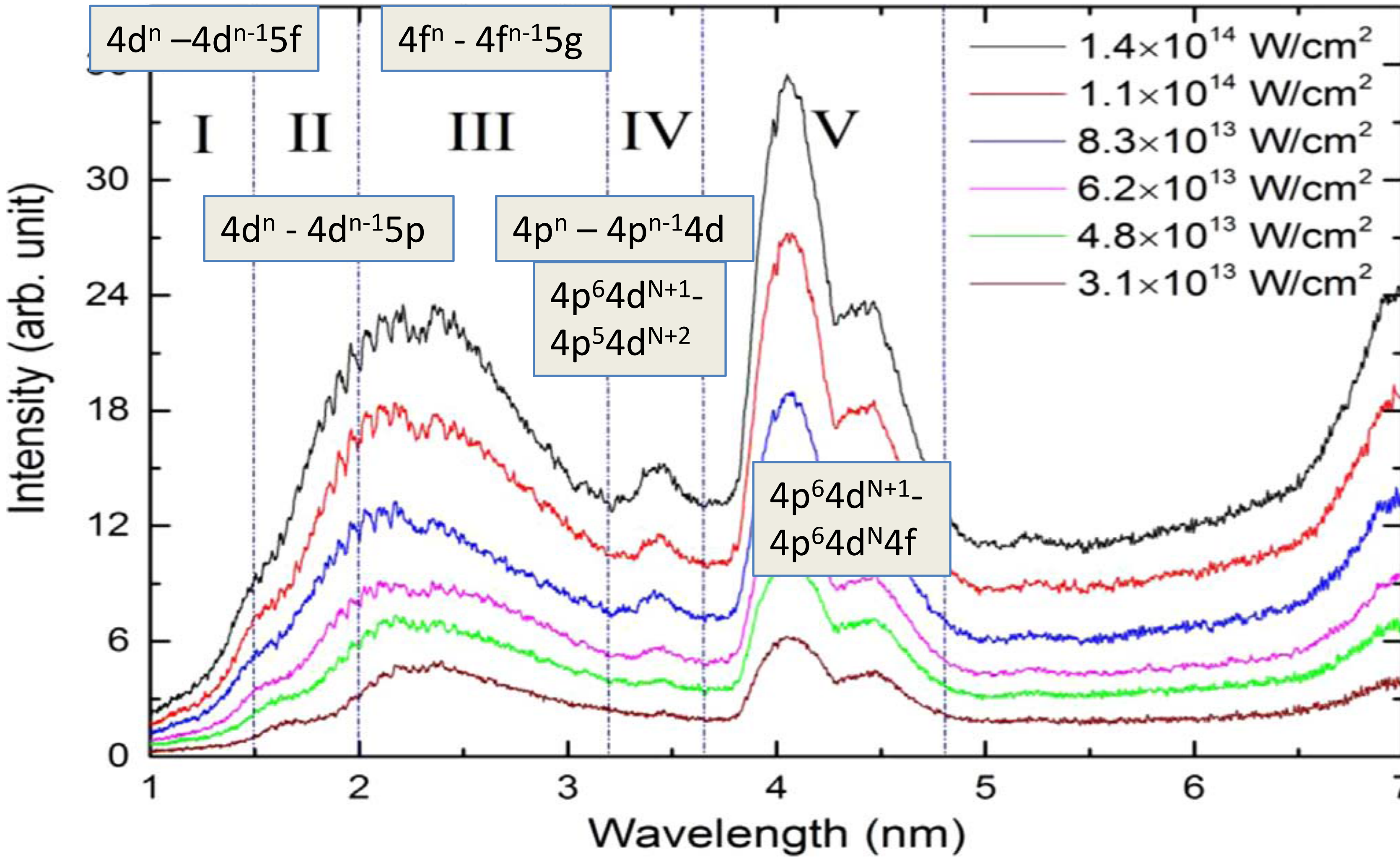

Outline

- Applications of Laser Produced Plasmas (LPPs) as Light Sources for Lithography and Microscopy.
- Properties of LPPs
- Properties of $\Delta n = 0$ UTAs
- Application of $\Delta n = 1$ UTAs
- Conclusions

Δn = 1 UTAs; Alternative WW Source

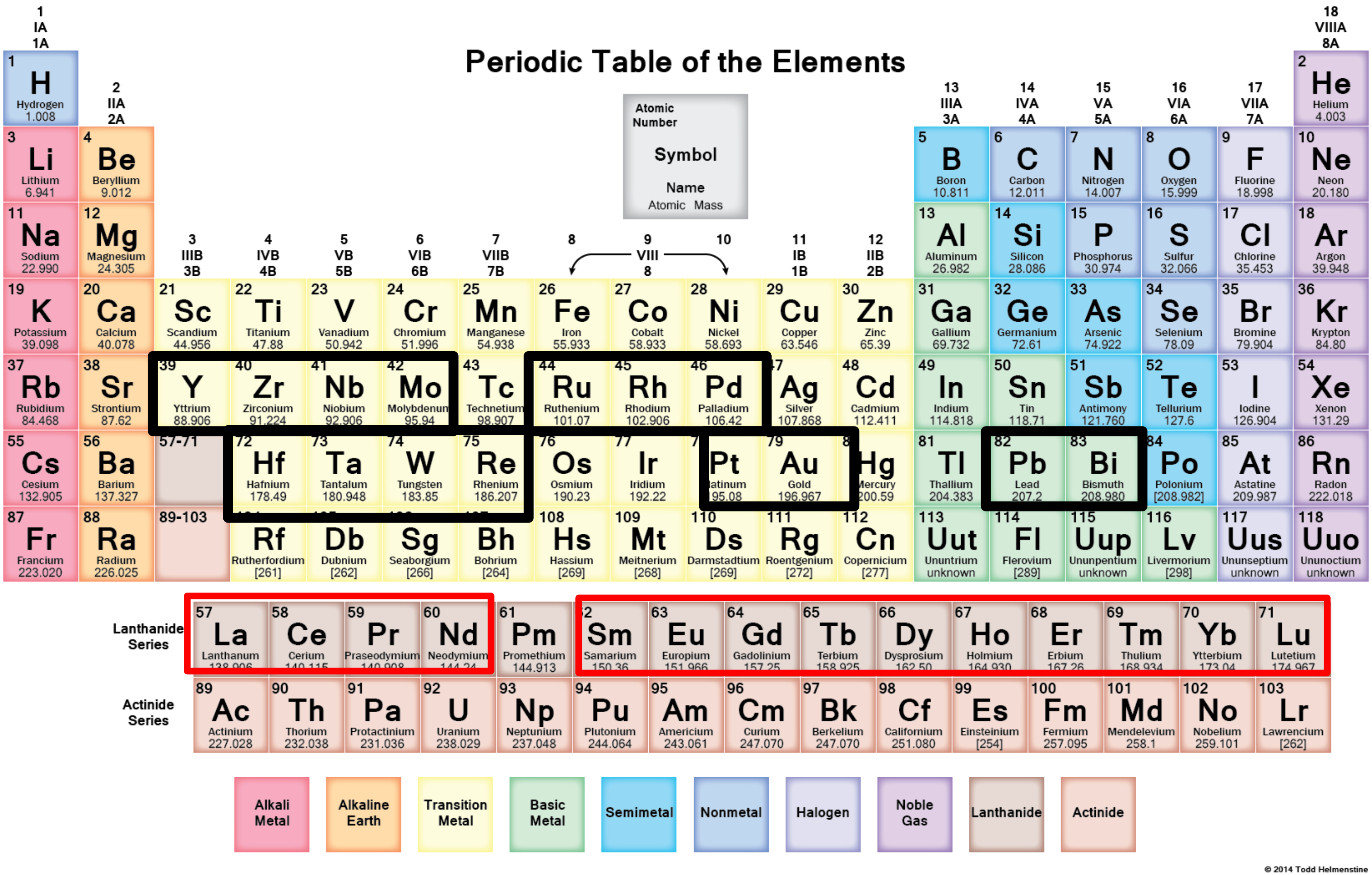

Δn=1 transitions in 2nd transition row

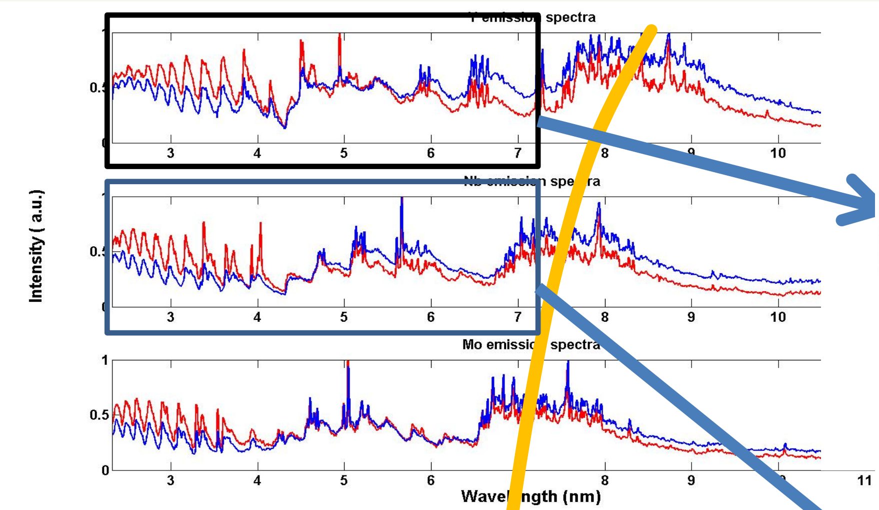

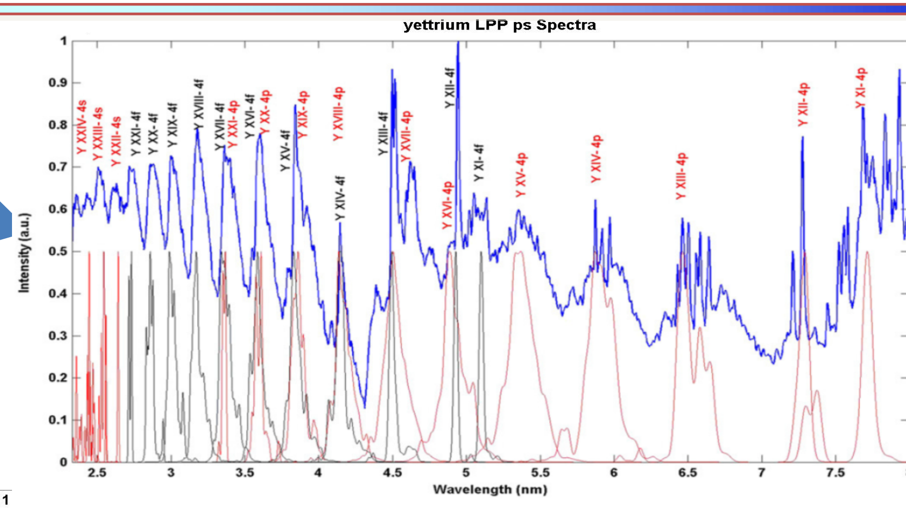

Δn=0, 3p-3d

Δn=1, 3d-4p and 3d-4f

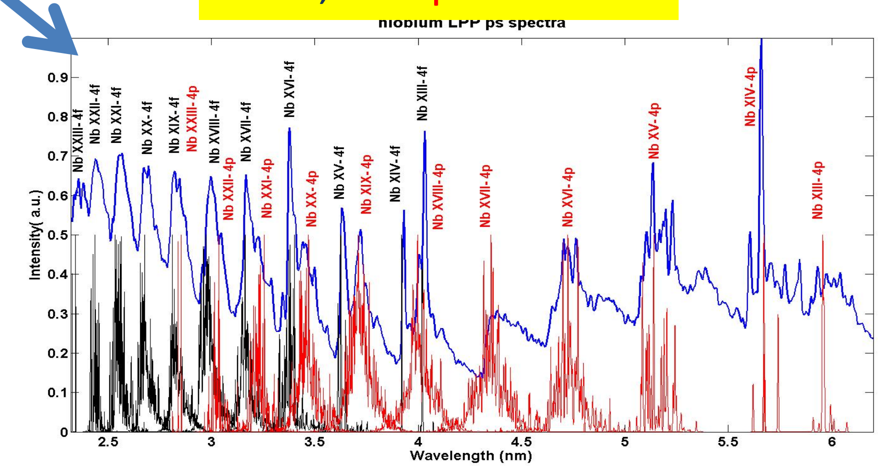

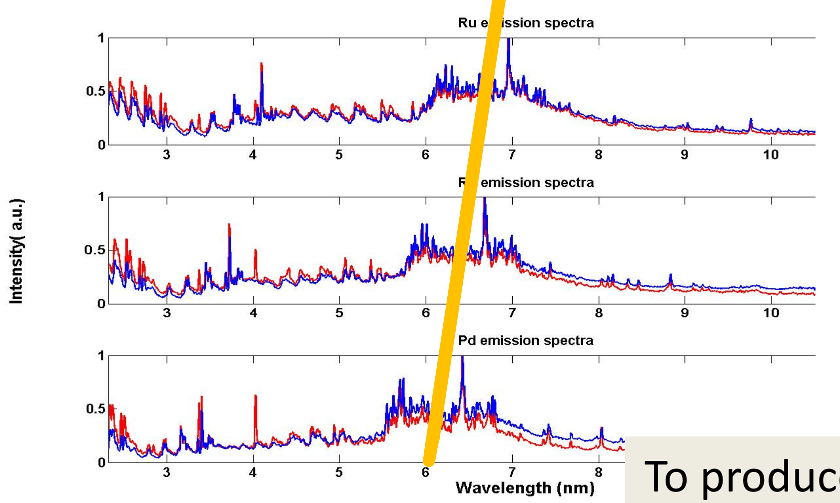

To produce the ion stages required (up to ~23+:
T_e ~300 eV, Φ~2×10^{12} Wcm^{-2}

Integrated Intensity in the Water Window due to different UTAs

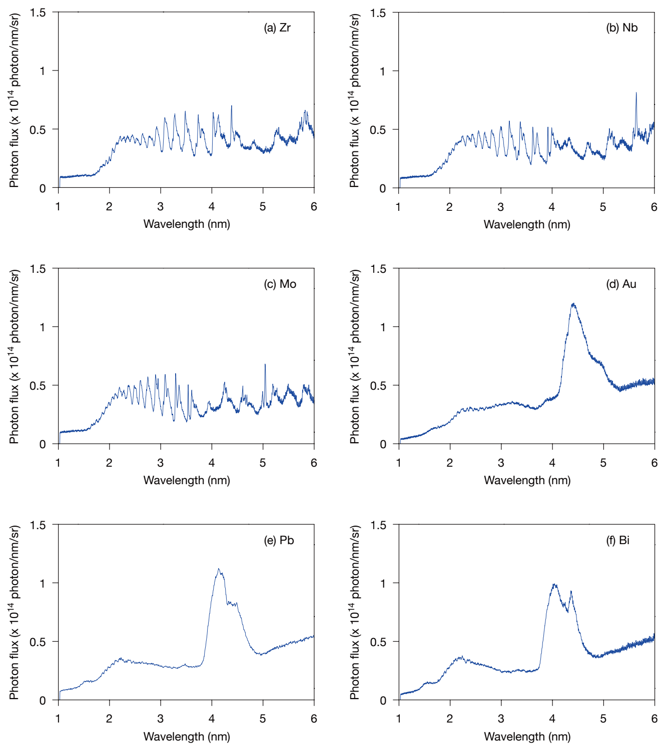

Comparison of the time-integrated emission spectra in the soft x-ray spectral region from laser-produced plasmas of Zr (a), Nb (b), Mo (c), Au (d), Pb (e), and Bi (f).

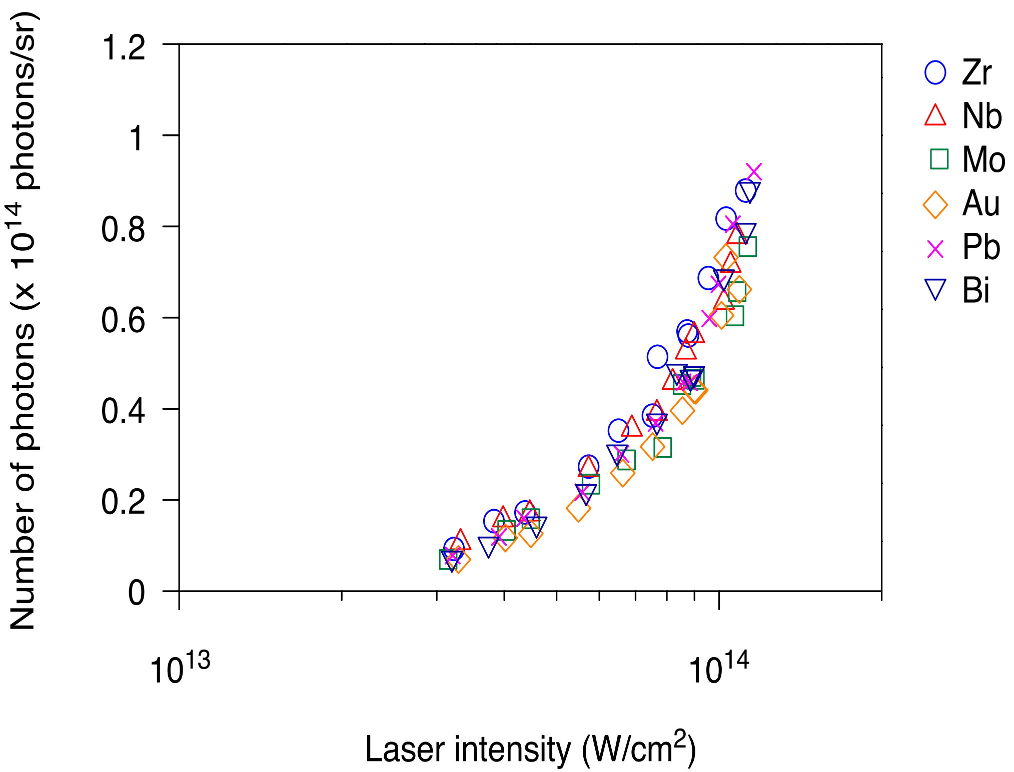

Laser power density dependence of the number of photons emitted in the water window

(Tamura et al. Opt. Letts.Vol. 43, No. 9, 2042)

Dual Laser Illumination of Mo

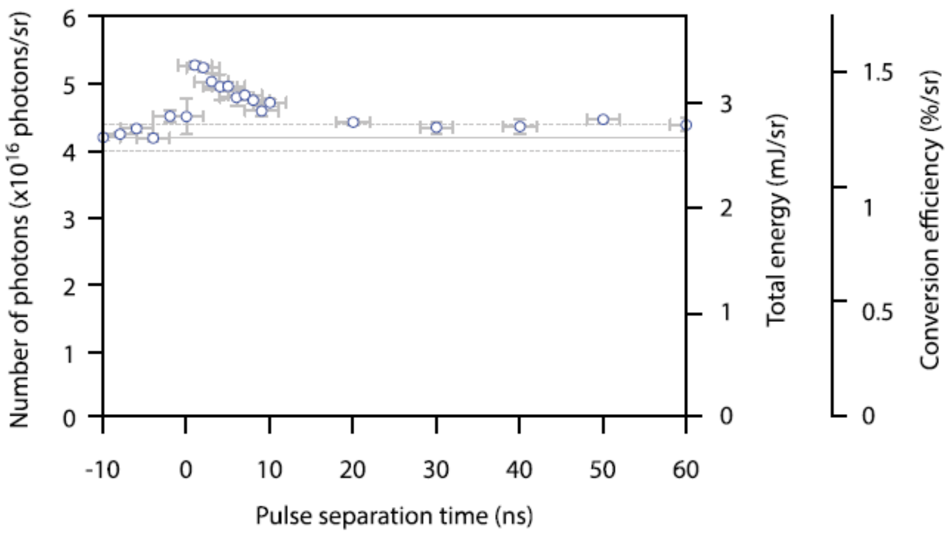

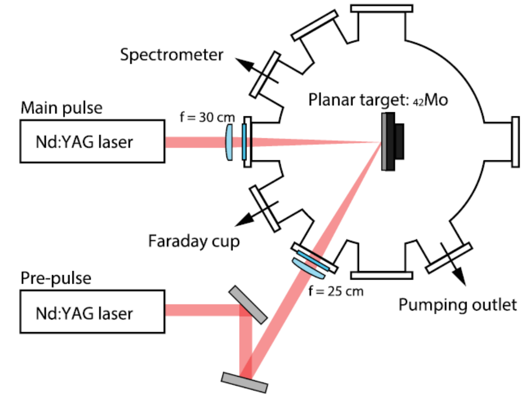

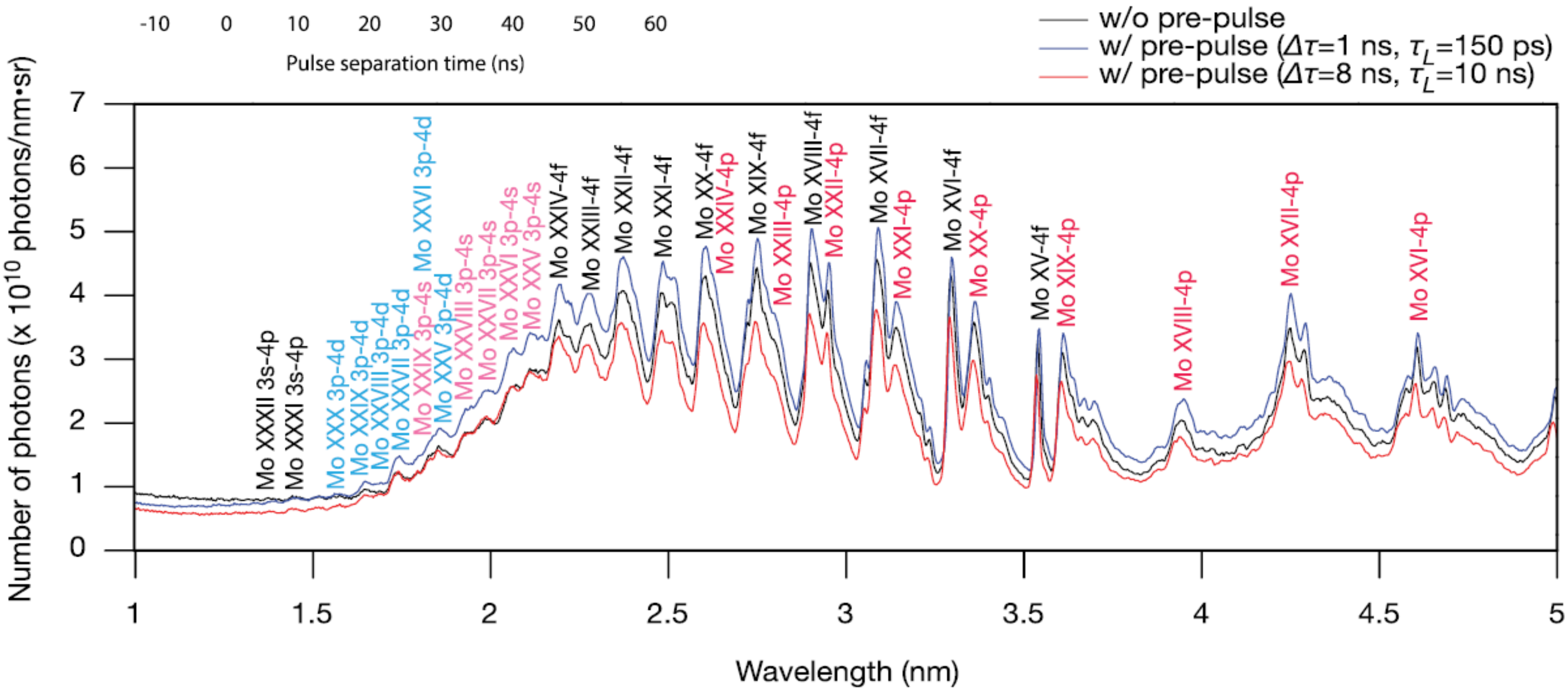

Conclusions

- Still more CE can be attained at 13.5 nm. Modelling needs more atomic data. A definitive line classification still does not exist.
- Solid state mid-IR lasers could give better beam profiles (spatially and temporally)
- Δn=1 transitions in medium and high Z elements and Δn=0 in high Z elements can be used for water window sources.
- Δn=1 transitions require less energy for excitation than Δn=0. Also some match existing MLMs and atomic data needed for optimisation
- Ideal source depends on mirror bandwidth. For very narrow bandwidth at low wavelength H-like 1s-2p line in low Z ions best. Water/ammonia/organic liquid droplet, dual ps pulse irradiation.

Thanks to:

Science Foundation Ireland Principal Investigator Grant 07/IN1/I1771

Enterprise Ireland

Intel Ireland and Intel Oregon

EACEA Erasmus Mundus Project EXTATIC framework partnership agreement FPA-2012-0033

Science Foundation Ireland International strategic collaboration award 13/ISCA/2846

University College Dublin

National Institute for Fusion Science

Utsunomiya University

JSPS, Japan Society for the promotion of Science KAKENHI grant 15H03759

Chinese Scholarship Council

National Natural Science Foundation of China, grant 11304235

Scientific Research Foundation of Hubei Province grant Q20131512

THANK YOU!